6. SITE 504[1]

Shipboard Scientific Party[2]

HOLE 504B

Date occupied: 7 April 1983

Date departed: 16 April 1983

Time on hole: 9 days, 10 hr., 1 min.

Position: 1°13.6′N; 83°43.8′W

Water depth (sea level; corrected m, echo-sounding): 3460 m[3]

Water depth (rig floor; corrected m, echo-sounding): 3470 m[3]

Bottom felt (m, drill pipe): 3473.5[3]

Penetration (m): None[4]

Principal results: A detailed temperature-measurement profile was completed from 78 to 449 m below seafloor (BSF), above and below an underpressured high permeability zone in the upper 100 m of basement of Hole 504B, by using both the hydraulic piston corer (HPC) temperature shoe and the Barnes/Uyeda tool. These data indicate that downhole flow has decreased from 25 m/hr. (measured on Leg 83 in November 1981) to 2 to 3 m/hr. The measurement of temperatures lower in the hole was complicated by sensor problems, but the temperatures indicate a gradient of 0.080°C/m in Layer 2C and bottom-hole temperatures of 160° to 165°C.

Four water samples were collected using the Barnes/Uyeda tool, and three samples were collected using the packer sampler go-devil. The hole was highly contaminated with drilling mud, but major-element water chemistry analyses done on board are reliable and show linear relations between Mg^{2+} and Ca^{2+} after the latter is corrected for the precipitation of anhydrite.

The completion of the oblique seismic experiment planned at the hole was made more difficult by recurrent leaks in the cable adaptor for the borehole seismometer. Nevertheless, we were able to conduct a complete shot pattern with the seismometer at 317 m BSF and 547 m BSF and partial shot patterns with the seismometer at 727 m BSF and 942 m BSF. We also completed a multichannel sonic log of the upper 150 m of basalt (Layer 2A, including the underpressured zone). The shape of the waveforms varies with the degree of fracturing indicated by previous borehole televiewer logs. A packer experiment run at 1056.5 m BSF failed because the rubber packer element was unable to withstand the high temperatures at the bottom of the hole.

In the intervals between the experiments we pumped 150,000 gal. of seawater to 4734 m below sea level (1270 m BSF), which we estimate removed 99% of the bentonite suspended in the borehole water (although bentonite caked on the walls of the hole would not have been affected).

BACKGROUND AND OBJECTIVES

Hole 504B, the deepest hole drilled into oceanic crust, was spudded during Leg 69 and deepened during Legs 70 and 83 to a total below sea level depth of 4823.5 m, 1350 m below the seafloor (BSF) and 1075.5 m into basaltic basement (Fig. 1). Because of its depth, Hole 504B provides earth scientists with a unique opportunity to study the geology, geophysics, and geochemistry of oceanic crust. It was to take advantage of this opportunity that the *Glomar Challenger* returned to the hole for 9 days at the end of Leg 92.

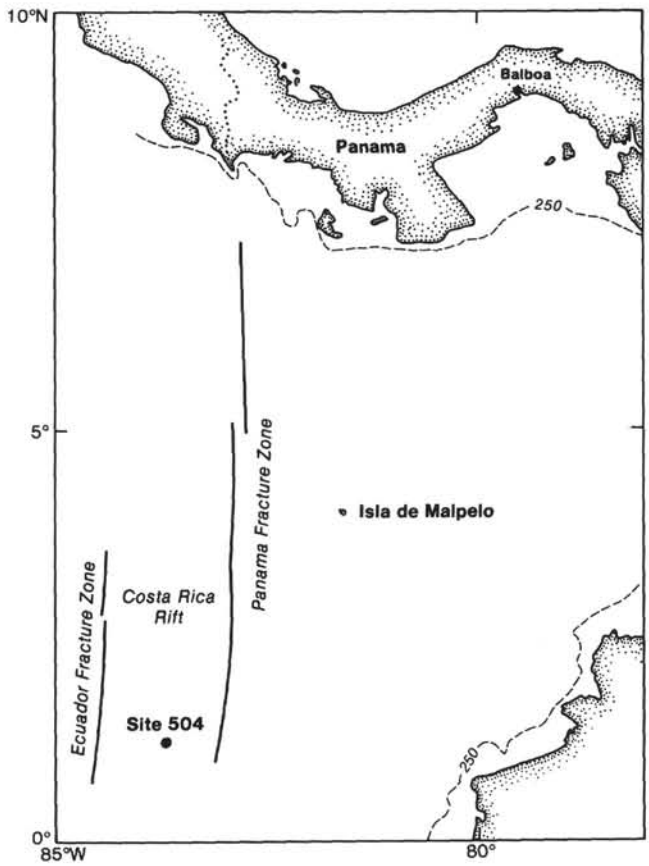

Figure 1. Location of Hole 504B in the eastern equatorial Pacific. Bathymetry in m.

[1] Leinen, M., Rea, D. K., et al., *Init. Repts. DSDP*, 92: Washington (U.S. Govt. Printing Office).

[2] Margaret Leinen (Co-Chief Scientist), The University of Rhode Island, Narragansett, Rhode Island; David K. Rea (Co-Chief Scientist), The University of Michigan, Ann Arbor, Michigan; Roger N. Anderson, Lamont-Doherty Geological Observatory, Palisades, New York; Keir Becker, Scripps Institution of Oceanography, La Jolla, California (present address: University of Miami, Miami, Florida); Jacques J. Boulègue, University of Paris, Paris, France; Jörg Erzinger, Justus-Liebig University, Giessen, Federal Republic of Germany; Joris M. Gieskes, Scripps Institution of Oceanography, La Jolla, California; David Goldberg, Lamont-Doherty Geological Observatory, Palisades, New York; Marjorie S. Goldfarb, Scripps Institution of Oceanography, La Jolla, California (present address: University of Washington, Seattle, Washington); Robert Goldsborough, Woods Hole Oceanographic Institution, Woods Hole, Massachusetts; Michael A. Hobart, Lamont-Doherty Geological Observatory, Palisades, New York; Miriam Kastner, Scripps Institution of Oceanography, La Jolla, California; Stephen Knüttel, Florida State University, Tallahassee, Florida; Mitchell W. Lyle, Oregon State University, Corvallis, Oregon; Tadashi Nishitani, Akita University, Akita, Japan; Robert M. Owen, The University of Michigan, Ann Arbor, Michigan; Julian A. Pearce, The Open University, Milton Keynes, United Kingdom (present address: The University, Newcastle-upon-Tyne, United Kingdom); Karen Romine, The University of Rhode Island, Kingston, Rhode Island (present address: Exxon Production Research Company, Houston, Texas); Ralph A. Stephen, Woods Hole Oceanographic Institution, Woods Hole, Massachusetts.

[3] From Volume 69 of the *Initial Reports* (Cann, Langseth, Honnorez, Von Herzen, White, et al., 1983).

[4] Downhole sampling and experiments only.

Our primary purpose in returning to Hole 504B was to conduct an oblique seismic refraction experiment, in which shots made in a spokes-and-circles pattern were to be recorded by a borehole seismometer. In 5 days we were to complete the shooting pattern with the receiver at four different depths chosen to include crustal Layers 2A, 2B, and 2C. The experiment was designed by Ralph Stephen of the Woods Hole Oceanographic Institution, who had developed a three-component borehole seismometer that could withstand the elevated temperatures of 150° to 160°C expected near the bottom of Hole 504B. We intended to rendezvous with Stephen aboard the *Ellen B. Scripps*, which would then function as the shooting ship for the seismic refraction experiment.

Hole 504B had been undisturbed for over 15 mo., since Leg 83 had departed late on New Year's Day, 1982. We were scheduled to arrive in April of 1983. The water temperature in the hole was therefore expected to have had time to approach steady-state conditions, and the water chemistry was expected to show signs of water–rock interaction. The measurement of downhole temperatures and the acquisition of water samples, although second in priority to the oblique seismic experiment, had to be performed before the water in the hole became disturbed, so the first planned operation at Hole 504B was to move the drill pipe down very slowly to minimize disturbance, acquiring water samples and making temperature measurements at a number of depths.

Other objectives were to acquire multichannel sonic (MCS) logs of the cooler part of the hole and to perform a deep packer experiment to test the bulk permeability of the lower portion of the hole (crustal Layer 2C).

OPERATIONS

Upon arrival at Hole 504B (at 1235 hr. on 7 April 1983), we dropped a 13.5-kHz beacon, retrieved the underway profiling gear, and positioned over the beacon. The 13.5-kHz beacon began to fade out, and the 16-kHz beacon we dropped to replace it did not work. The third beacon we dropped (also 16 kHz) functioned properly, and the vessel was operating in the automatic mode by 2025 hr. Scanning for the Hole 504B re-entry cone began at 0107 hr. on 8 April; the cone was spotted at 0156 hr. After verifying its presence we searched for the Hole 504A cone, which was supposed to lie 300 m to the west, to make sure that we were at the correct location. Once that cone was found, the ship returned to Hole 504B, and re-entry was effected at 0706 hr. The sampling program began by 0900 hr. on 8 April.

Because of the number and variety of the tools to be used in this hole and the need to ensure that there would be enough time to meet all scientific objectives, we used a special bottom-hole assembly (BHA). The BHA was terminated with a cleanout bit. A standard support bearing was bored out to 3.675 in., which allowed sufficient clearance for the borehole seismometer tools yet left sufficient shoulder material to land the *in situ* pore water sampler/heat flow barrels, the large-volume water sampler, and the packer safety go-devil. Finally the Lynes drill pipe packer was made up directly above the bit. The size of the landing shoulder was marginal, so we used new landing subs and watched them carefully, replacing them occasionally with other new subs. This configuration allowed us to complete all of the Hole 504B operations on one pipe trip and one re-entry, saving time that was needed later to complete the scientific objectives.

The water sampling and temperature measurement program (Table 1) resulted in the recovery of water samples at seven depths and temperature measurements at 25 depths down to 1204 m BSF. After completing the sampling program, we lowered the drill pipe further to determine whether the hole was open to the total depth drilled on Leg 83. We found an impenetrable bridge at 4744 m (1270.5 m BSF). We then pulled the pipe back to 3624 m and rigged logging sheaves. The borehole seismometer began running in the hole at 0630 hr. on 10 April.

The oblique seismic experiment was an ordeal. The primary difficulty was that we did not have the two connectors necessary to link the Schlumberger head on the seismometer to the Gearhart–Owen logging cable. The DSDP support group at Scripps, although it had assumed responsibility for providing this equipment, had provided neither the connectors nor all the parts necessary to construct them. As a result, the connections between the tool and the cable flooded six times. We made a continuous 7-day effort to redesign, rebuild, and refit the cable-head adaptor. Several of those on board worked continuously for more than 24 hr., and the delay ended up costing both the *Glomar Challenger* and the *Ellen B. Scripps* at least 3 days of ship time. In between the floods and the failures for other reasons, the seismometer collected high quality data sets from (below rig floor) depths of 3790, 4020, 4200, and 4415 m before failing, presumably from extreme temperatures, at the deepest setting (4705 m). Despite these difficulties, however, this was the most extensive borehole oblique seismic experiment ever conducted. The tool came on deck for the last time at 1359 hr. on 16 April.

We completed three other downhole operations between the seismometer lowerings. Two separate multichannel sonic logs were acquired for the upper 150 m of the basement; the runs lasted about 6 hr. each and were made on the 14th and 15th of April. The tool worked well both times, but the data acquisition system on deck did not record the data on the disk properly the first time. For the second run the oscilloscope image of the waveforms was recorded on Polaroid film and videotape for later digitization. A deep packer experiment, conducted from 1845 to 2330 hr. on 14 April, was not successful. When the packer element arrived on deck late on the 16th, it consisted only of the metal webbing, and all the exterior rubber was gone. It seems clear that a unit capable of withstanding high temperatures will be required to conduct packer experiments in 160°C water.

For several hours on the 14th and 15th of April we pumped seawater down to 4734 m (1260.5 m BSF), 10 m above the bridge at 4744 m, in an attempt to flush suspended bentonite (drilling mud) from the hole. During this time we pumped a total of 150,000 gal. of water

Table 1. Geochemistry–heat flow program, Hole 504B.

Depth below rig floor (m)	Depth (m BSF)	Tool(s) deployed: Von Herzen HPC heat flow shoe	Barnes/ Uyeda heat flow sampler	Maximum-reading thermometer	Barnes/Uyeda *in situ* pore water sampler	Large-volume (go-devil) water sampler
Run 1						
3551	78	✓	✓			
3580	107	✓	✓			
3609	135	✓	✓			
3638	164	✓	✓			
3666	193	✓	✓			
3695	221	✓	✓			
3724	250	✓	✓			
3752	279	✓	✓			
3781	307	✓	✓			
3809	336	✓	✓			
3838	364	✓	✓			
3866	393	✓	✓		✓[a]	
3894	421	✓	✓			
3923	449	✓	✓			
Run 2						
3980	507		✓			
4009	535		✓			
4037	564		✓		✓	
Run 3						
4066	592		✓			
4094	621		✓			
4123	650		✓		✓	
4152	679		✓			
Run 4						
4210	736		✓		✓	
4238	765		✓			
4267	794		✓	✓		
Run 5						
4400	926					✓
Run 6						
4478	1004		✓			✓
4507	1033		✓	✓		
Run 7						
4526	1052		✓	✓		
Run 8						
4572	1099			✓		✓
Run 9						
4621	1148			✓		
Run 10						
4678	1024			✓		✓

[a] Sampler failed to trigger.

down the hole, 6.8 times the calculated volume of the hole. If we assume that contamination was reduced by 50% by each flushing, less than 1% of the original suspended mud remains. Since the process does not remove bentonite caked on the walls, however, it will never be possible to determine how much the remaining bentonite has affected the future chemical alteration of the rock or seawater.

Leg 92 completed pulling out of Hole 504B (bit was on deck) at 2215 hr. on the 16th of April, 1983. We were under way for Balboa, Panama at 2236 hr.

COMPOSITION OF DRILLING MUDS (PRELIMINARY RESULTS)

Muddy water was recovered at the three large-volume (go-devil) sample depths of 926, 1100, and 1204 m BSF

in Hole 504B. The mud-to-water ratio increased with depth.

In order to investigate the nature and extent of the reactions between the hot water and the mud, the drilling bentonite from supplies on board the *Glomar Challenger* for Leg 92 (which, according to Mike Storms, Operations Manager, was the same drilling mud as used on Leg 83) and the mud samples recovered from the go-devil sampler were analyzed by petrographic microscopy and X-ray diffraction (XRD). The mud samples analyzed were GDW-I-5 (first go-devil depth [926 m], barrel 5); GDW-II-5 (second go-devil depth [1100 m], barrel 5); and GDW-III-4 and GDW-III-5 (third go-devil depth [1204 m], barrels 4 and 5). Smear and XRD slides of both bulk and coarse fractions (coarse silt and sand) were analyzed. XRD data from glycolated (with glycerol) samples were also obtained.

Results

All the mud samples recovered from the hole are different from and darker in color than the shipboard bentonite (Table 2). Iron–manganese oxyhydroxide, which occurs as coatings on pre-existing phases and as discrete particles, is presumed to be responsible for the brown colors; dark volcanic glass and magnetite derived from the walls of the hole may be responsible for the black color.

The bentonite is composed mainly of smectites, with some quartz and feldspars, traces of mica grains, small amounts of barite, and traces of oxyhydroxides. Volcanic glass, some brown and some colorless, composes 3 to 5% of the bentonite. The brown glass grains are coarser than the colorless grains. Two additional, as yet unidentified, minor components are also present. The quartz-to-feldspar ratio is higher in the coarse fraction than in the bulk sample.

Samples GDW-I-5, GDW-III-4, and GDW-III-5 are generally similar mineralogically. Smectite is the major constituent; the samples contain more iron–manganese oxyhydroxides, mostly fine grained, than the bentonite, distinctly less volcanic glass, less quartz, and much less feldspar. Barite was observed only in the deepest sample (GDW-III-5).

There are, however, some important differences between Sample GDW-I-5 and the deepest go-devil samples (GDW-III-4 and GDW-III-5). The size of the coarse fraction, and thus the concentration of quartz, feldspar (± volcanic glass), and iron–manganese oxyhydroxides (and barite), is significantly greater in the two lowest samples, and it is greatest in GDW-III-5. In addition, anhydrite, which we presume formed by reactions in the borehole, is present in only trace quantities in Sample GDW-I-5, but it is an important phase (up to a few percent) in Samples GDW-III-4 and especially in GDW-III-5.

Table 2. Color of bentonite and mud samples from Hole 504B.

Sample	Color
Bentonite	Pale olive 5 Y 6/3
GDW-I-5	Olive brown 2.5 Y 4/4
GDW-II-5	Black 10 YR 2.5/1
GDW-III-4	Dark yellowish brown 10 YR 4/4
GDW-III-5	Dark yellowish brown 10 YR 4/4

Note: Colors are according to the Munsell soil color chart.

Sample GDW-II-5, a black mud, although coarser grained than even Sample GDW-III-5, is composed primarily of smectite. Iron–manganese oxyhydroxides are moderately abundant as fine disseminated particles (as in GDW-I-5) but are even more common as coarser particles; they compose about 50% of the coarse fraction. This fraction also contains considerably more volcanic glass than the other mud samples. In addition to brown and some colorless glass, green glass is present, although it is not very common. Only traces of quartz and feldspars were observed. This sample contains some magnetite, but no anhydrite was detected.

The bentonite and each of the mud samples exhibit a different glycolated smectite peak. Coccoliths were recognized in the mud samples. In Sample GDW-III-4, for example, a species of *Gephyrocapsa*, an extant genus, was present.

Summary and Discussion

The muds recovered by the go-devil sampler at 926, 1100, and 1204 m BSF (at temperatures from 135° to 155°C) differ from the original drilling bentonite as follows:

1. The mud samples contain considerably less volcanic glass than the bentonite.
2. The mud samples are highly enriched in iron and manganese oxyhydroxides relative to the bentonite.
3. Compared with the bentonite, the mud samples, even the deepest sample (GDW-III-5), contain much less quartz and even less feldspar.
4. X-ray diffraction analyses indicate downhole changes in the smectites. The smectite in the mud samples also differs from that in the bentonite.
5. Anhydrite is present only in the mud samples, in particular in the deepest and hottest sample (GDW-III-5). It is absent in the bentonite sample from the ship.

The reactions postulated in the borehole would remove Ca^{2+}, SO_4^{2-}, Na^+, iron, and manganese from seawater and release silica and some Ca^{2+} to the solution. (Although not evident from this preliminary study, at least some dissolved Mg^{2+} must have been removed by the smectites as well.)

The effect of the presence of bentonite on the interaction between seawater and Layer 2 is difficult to evaluate, since the trends that result from reactions between seawater and ocean crust could be very similar to those that result from reactions between seawater and bentonite.

OBLIQUE SEISMIC EXPERIMENT

The objective of performing the borehole seismic experiment was to learn about the velocity–depth structure, seismic anisotropy, heterogeneity, and attenuation of Layer 2 in young oceanic crust. The information obtained in this oblique seismic experiment (OSE) is on a scale of hundreds of meters, and, when compared with the extensive smaller scale downhole logging measure-

ments made at Hole 504B, it provides a rare synoptic view of physical rock properties and large-scale seismic structure.

The oblique seismic experiment entails clamping a three-axis seismometer at various depths down a borehole, generating a series of explosions in a known pattern at the sea surface (Fig. 2), and recording arrival times and amplitudes for each shot. The data can then be used to determine the details (resolution: 100 m) of the velocity–depth structure, the attenuation of the upper oceanic crust, the presence and orientation of seismic anisotropy, and the degree of lateral heterogeneity. The results of the experiment, when coupled with an examination of the recovered rock and the measurement of various downhole properties (such as porosity, sonic velocity, crack density, and resistivity) can help reveal the relationship of large-scale seismic velocity to *in situ* borehole mineralogy and crack structure, the type and significance of anisotropy, if any, and the relationship of any such anisotropy to crack orientation and the crustal formation process.

The successful completion of three previous oblique seismic experiments (Fig. 3: south of the Bermuda Rise on Leg 52 [Stephen, 1978, 1979; Stephen et al., 1980a, 1980b]; in the Tamayo Fracture Zone area on Leg 65 [Stephen et al., 1983]; and near the Costa Rica Rift in Hole 504B on Leg 70 [Stephen, 1983; Stephen and Harding, 1983]) has proven the value of such experiments. In the Bermuda Rise experiment, good quality three-component amplitude and traveltime data helped produce velocity–depth functions for both compressional and shear waves. Polarization analysis of the data revealed the shear wave splitting indicative of seismic anisotropy (Stephen, 1981). The Tamayo Fracture Zone experiment collected only vertical-component data, but synthetic seismogram analysis (Stephen, 1977; Stephen et al., 1983) produced a well constrained velocity–depth function. The previous (Leg 70) oblique seismic experiment in Hole 504B obtained only traveltime data because the seismometer failed when it encountered the high (120°C) temperature in the borehole. A velocity–depth function was determined from the traveltime data alone (from two ocean-bottom hydrophones and two borehole geophone positions), but the lack of amplitude data precluded the synthetic seismogram modeling that would have further constrained the velocity–depth function.

On Leg 92, the three-component borehole geophone was clamped at four depths spaced approximately 200 m

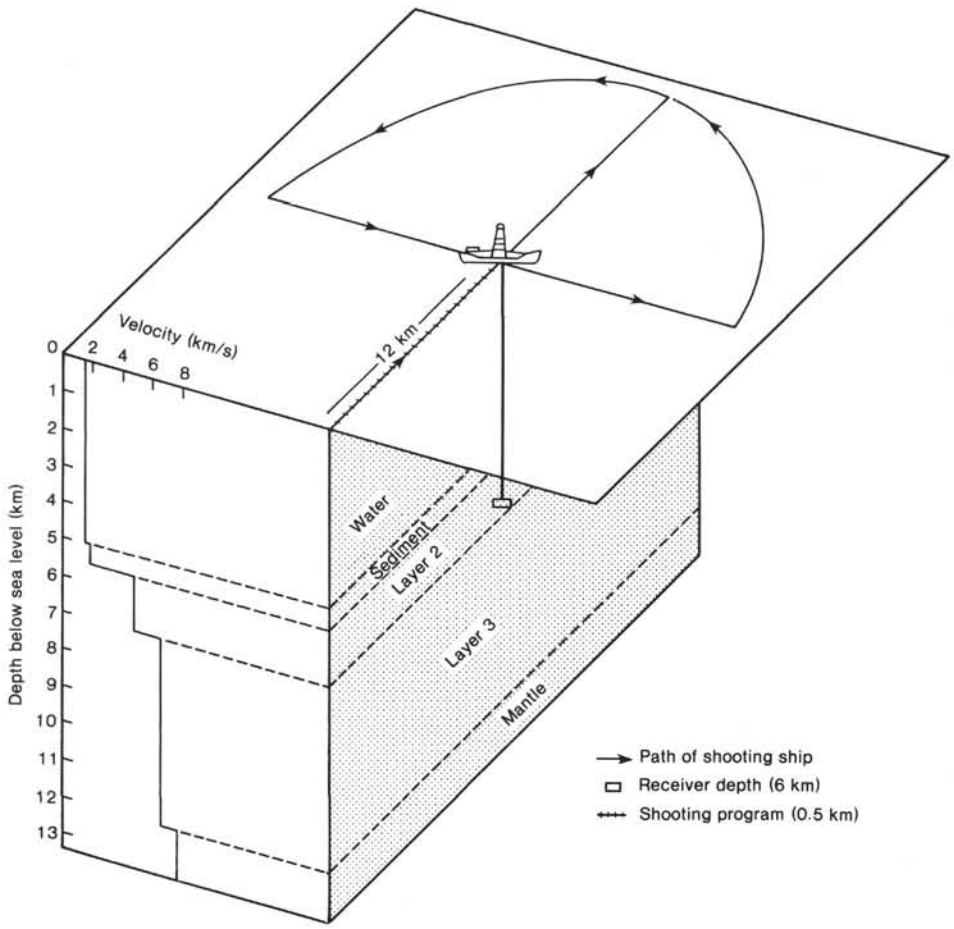

Figure 2. Schematic diagram of an oblique seismic experiment over oceanic crust. Schematic shows generalized changes in velocity. On Leg 92 a three-component borehole seismometer was deployed at four depths in basement, and almost 1000 charges were fired on radial lines and concentric circles about the hole within a radius of 8 km.

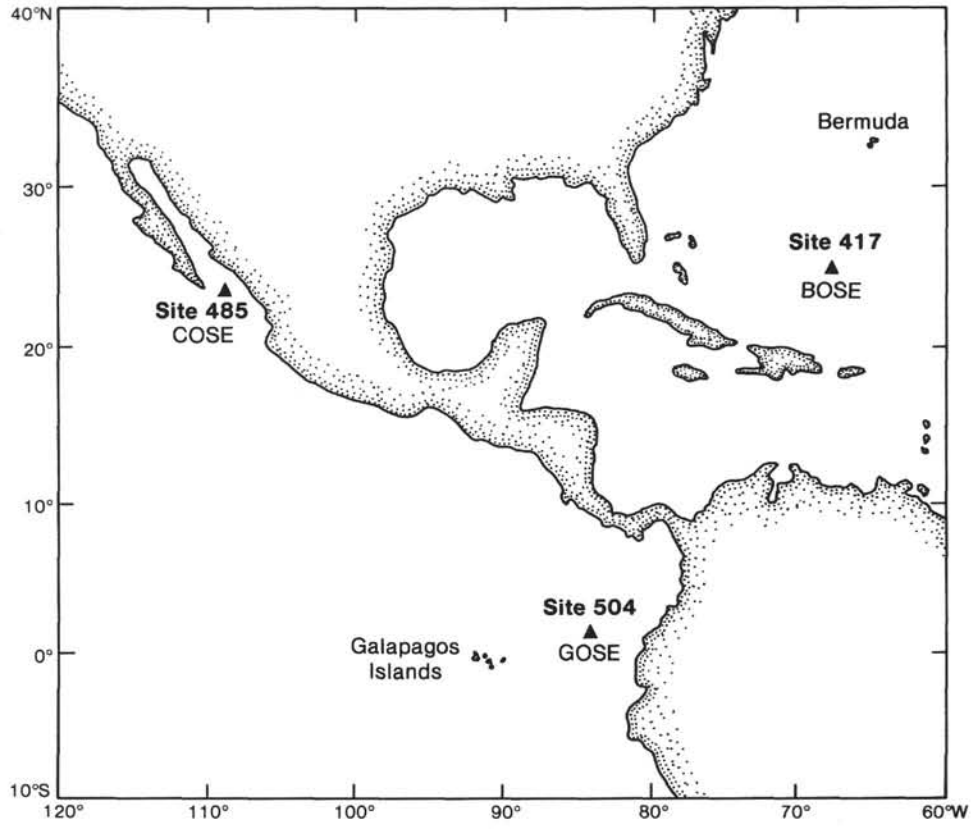

Figure 3. Locations of the three previous borehole seismic experiments: the Bermuda oblique seismic experiment (BOSE) on DSDP Leg 52, the California oblique seismic experiment (COSE) on DSDP Leg 65, and the Galapagos oblique seismic experiment (GOSE) on DSDP Leg 70. The Leg 70 experiment at Site 504 obtained only traveltime data; the Leg 92 experiment at the same site obtained a much more complete data set.

apart: 3780, 4010, 4190, and 4405 m below sea level (BSL), or equivalently 42, 272, 452, and 667 m into basement. The high temperatures (up to 160°C) in Hole 504B, which caused the Leg 70 borehole seismometer to fail, necessitated the use of a new seismometer designed and tested for temperatures up to 200°C. The basic unit was a WLS-1100 wall-lock seismometer purchased from Geo-Space Corp. This unit was modified by the Woods Hole Oceanographic Institution with a variable-gain, three-component seismometer. While the *Glomar Challenger* maintained its position, the shooting ship *Ellen B. Scripps* sailed a series of radial lines and concentric circles centered on the hole, firing 7-kg shots every 0.5 km out to a distance of 8 km. This firing sequence was repeated with the geophone at each depth, with varying degrees of success. The failure of the adaptor that connects the Gearhart-Owen logging head to the Schlumberger head on the borehole seismometer prevented the successful collection of all 1600 planned shot records. Despite the repeated flooding of this connector, 994 shots were fired, and three-component true amplitude data were recorded on magnetic tape and ultraviolet paper. The data and an initial analysis are presented by Little and Stephen (1985).

In conclusion, the Leg 92 oblique seismic experiment was the most intensive borehole seismic experiment ever undertaken over oceanic crust (four geophone depths and 994 shots). In its lowest position (4415 m below rig floor), the geophone acquired the deepest borehole seismic data ever collected in oceanic crust, and it encountered the highest temperature (about 160°C) at which a borehole seismometer has ever remained functioning in oceanic crust.

BOREHOLE WATER STUDIES

A number of studies of the chemistry of the interstitial waters collected during the Deep Sea Drilling Project have suggested that some changes in the composition of these fluids are the result of the low-temperature alteration of the underlying basalts of Layer 2. These basalts are a sink for potassium, magnesium, sodium, and ^{18}O (H_2O) as well as a source of calcium (Lawrence et al., 1975; Lawrence and Gieskes, 1981; Gieskes and Lawrence, 1981; Gieskes, 1983). McDuff (1981) has argued that to maintain these concentration gradients, the large-scale circulation of formation waters must occur in ocean crust until it reaches an age considerably greater than that at which the so-called sealing of the crust occurs (Anderson and Hobart, 1976). This sealing occurs largely as a result of the accumulation of a thick sediment cover, impermeable to advection, so that transport of ions from Layer 2 through the sediments becomes diffusive (McDuff, 1981).

Hitherto there have been few opportunities to study the chemistry of the formation waters of the basalts to test some of the ideas developed on the basis of intersti-

tial water data. More direct inferences about the nature of formation waters were made possible during Legs 69, 70, and 83 with the go-devil packer sampler working in an active mode (Anderson, Honnorez, Becker, et al., 1985, pp. 47–48). Although contamination with freshly introduced seawater from the drill pipe was evident, the data obtained did suggest that the composition of formation waters was similar to that of the pore waters of the basal sediments of Site 504.

Studies carried out during Leg 83, when Hole 504B was deepened, indicated that the composition of the borehole waters had been changed greatly by the introduction of surface seawater into the hole during Leg 70 about 2 yr. before. Water was sampled at two depths during Leg 83: about 460 m BSF (80°C) and about 790 m BSF (116°C). Mottl et al. (1985) concluded that the end member concentrations of these samples, when corrected for contamination by the bottom waters during Leg 70, were as follows:

Depth (m BSF)	T (°C)	Ca^{2+} (mM)	Mg^{2+} (mM)	K^+ (mM)	Si (mM)	$^{87}Sr/^{86}Sr$	SO_4 (mM)
≈460	80	29	40	8.6	0.8	<0.7088	24.6
≈790	116	48	22	6.7	1.9	<0.7080	15

The differences in concentration between the two samples were interpreted in terms of the interaction between the drill hole water and the surrounding rock at the temperatures encountered, because at both the 80° and 116°C isotherms the inflow of bottom water was thought to be negligible. Thus, the prevailing conditions provided what amounted to a natural rock–seawater interaction experiment.

Whereas the Leg 83 experiments were carried out under relatively clean hole conditions, Leg 83 left drilling mud in the hole, as is evident from the large amount of bentonite retrieved from the bottom of the hole. As a result, the water studies carried out during Leg 92 represent not only basalt–seawater interactions but also bentonite–seawater interactions. Leg 92 visited Hole 504B about 15 mo. after Leg 83, a period somewhat shorter than the 23 mo. between Legs 70 and 83.

Hole Conditions and Operations

Because the time available was limited, we decided not to use the large-volume water sampler until we reached greater depths (and therefore temperatures) than on Leg 83. However, three successful runs were made with the Barnes/Uyeda water sampler (Fig. 4) at 564 m BSF (91.5°C), 650 m BSF (101°C), and 736 m BSF (108°C). We sent this tool down the pipe in a free fall. After it reached the bottom of the pipe, we slowly lowered the pipe by <50 m. We followed this procedure to ensure that we were sampling downhole water and not water pushed down the hole by the tool during its descent in the pipe. We could not use this procedure with the go-devil packer sampler, however, because this tool is lowered on the sandline. Lowered in this manner, this sampler can seriously contaminate the borehole water, because it is 20 m long and pushes down a considerable plug of bottom water or a mixture of bottom seawater and borehole waters from higher levels. This plug will then mix with true *in situ* borehole water in an undetermined fashion (see the sections on bottom-water contamination).

The first go-devil run, which took samples at 926 m BSF (127°C), suggested that we would have problems with drilling mud that would be more severe at greater depths. Typically the sample barrels contained large amounts of bentonite as well as iron oxyhydroxides. The borehole water had to be separated from the bentonite by careful decantation and filtration. The bentonite contamination grew worse at 1099 m BSF (141°C), and at 1204 m (150°C) a thick slurry was recovered. The water samples for chemical analysis from the last two go-devil runs were obtained by centrifugation and subsequent filtration.

Sample Treatment

Most slurry samples were immediately acidified with nitric acid to prevent the precipitation of iron oxyhydroxides and stored for future work (about 1 ml of concentrated HNO_3 was used for a 250-ml sample). Some nonacidified samples were also taken for the comparison of trace metals. Samples of bentonite, pipe dope, lubriplate grease, and so forth were also collected for contamination studies.

Samples for the analysis of dissolved silica were obtained from the various sample bottles after filtration and stored in plastic vials. However, the silica values may not be representative of *in situ* values, because interaction with bentonite may have taken place after sampling at temperatures lower than *in situ* temperatures. Samples from the Barnes/Uyeda tool were analyzed after the titration of these samples for alkalinity.

The methods used for major-element analyses were as follows: calcium and magnesium—titrations, Wescan ion chromatography; potassium—Wescan ion chromatography; lithium—Wescan ion chromatography; sulfate—Wescan ion chromatography; minor constituents (H_4SiO_4, NH_4+, NO_3-)—colorimetry; chloride, sulfide, reduced sulfur—potentiometry. Alkalinity was also determined by potentiometric titration. (Alkalinity samples were stored for further work in the shore laboratory, but this chapter addresses the shipboard chemistry only.)

Before discussing the analysis results, we will consider the contamination of the borehole water by the sampling equipment and by the water introduced from higher levels (mostly bottom seawater).

Contamination

Nitrate as an Indicator of Bottom-Water Contamination

Mottl et al. (1985) point out that nitrate is a good indicator of contamination by bottom water, because at the high-temperature, reducing conditions present in the hole, nitrate would normally be absent. Nitrate is absent from surface seawater, but bottom water has an NO_3^- concentration of about 39 μM. The temperature profile

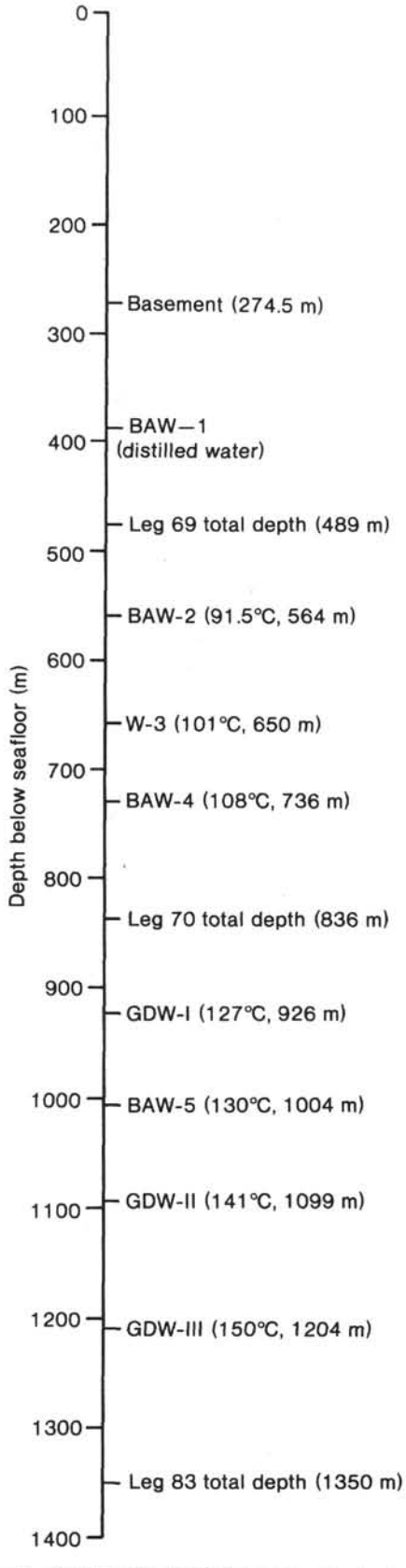

Figure 4. Depth of Hole 504B (Leg 92) samples. *In situ* temperatures were estimated from the Leg 70 gradient of 0.114°C/m, shown on Figure 10. BAW-1 failed to trigger, and still contained distilled water.

for the upper part of this hole, below the casing, showed signs of bottom-water flow-in, and the samples from GDW-I (Fig. 4) showed appreciable quantities of nitrate. Moreover, the Barnes/Uyeda sample taken below GDW-I (BAW-5) contained as much as 35 μM nitrate (90% of bottom-water concentration). We presume that these high values result from downhole contamination by bottom water, although the route from the seafloor to the sampling device is obscure.

If reduced substances (e.g., Fe^{2+}, reduced sulfur species) are present in the hole, however, reactions with NO_3^- may have occurred that would hamper the use of NO_3^- as an indicator of contamination. There is experimental evidence in support of the operation of this process (J. Boulègue and F. Morel, pers. comm., 1983). The absence of correlation between Ca^{2+} and NO_3^- (Fig. 5) also indicates that nitrate content is of limited usefulness as an indicator of bottom-water contribution. The go-devil samples from the lowest two depths show very small nitrate values, but these samples may have been affected by reduction, particularly the samples from GDW-II, which have appreciable concentrations of reduced sulfur species. Thus, the lack of NO_3^- cannot be used as *a priori* evidence that a sample is uncontaminated.

Chloride Contents as an Indicator of Bottom-Water Contamination

Except in the samples from GDW-III, chloride content is remarkably constant at a level well within 1% of the bottom-water concentration (554 mM). Surface water has chlorinities of about 534 mM, so surface-water contamination should readily be apparent. Sample GDW-III-3 has a low chlorinity value, but we have reason to believe that the extremely high iron content of this sample caused problems with the titration. Samples GDW-III-4 and GDW-III-5 are somewhat high in Cl (about 1.6 to 2.2% higher than bottom water).

After surface water was introduced during the Leg 83 sampling, one of the Leg 83 go-devil samples (PA-3 of Mottl et al., 1985) had a chloride content of about 529

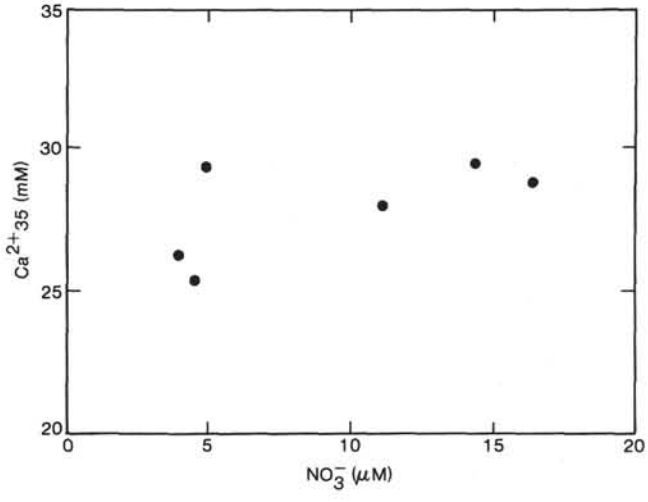

Figure 5. Nitrate–calcium correlation for GDW-I.

± 4 mM, a value close to the surface-water value of 533 mM. However, our data indicate that since then chlorinities have risen to values equal to those of bottom waters (554 mM): the samples from BAW-2 to BAW-4 (which have no nitrate) have a chloride content of about 554 mM. The rise in values can best be explained by the gradual downward mixing of bottom waters continuously introduced in the upper part of the hole. As temperature increases downhole, water density gradually decreases, and thus mixing should occur between the borehole and the overlying waters. It seem clear that a period of 15 mo. is sufficient to eradicate any remnant signal of surface-water chlorinities. In view of the rather constant Cl^- concentration, we assume that contamination by surface seawater was minimal.

The Barnes/Uyeda BAW-2 to BAW-4 samples do show bottom-water chlorinities. Nitrate concentration, on the other hand, is at not the bottom-water value but zero, evidence not only that nitrate in the deeper parts of the hole will be reduced but also that any nitrate detected deeper than these samples must represent contamination from the top of the hole.

The rather uniformly high downhole Cl^- concentrations rule out significant surface-water contamination, and the high NO_3^- values in the samples from GDW-I indicate contamination from bottom water. Thus, real major-ion concentration changes may be larger than estimated, although the absence of a NO_3^-–Ca^{2+} correlation indicates that no proper extrapolation can be carried out. However, the correlations between Ca^{2+} and Mg^{2+} and other ions will remain valid as long as the processes that affect the formation waters are similar at all levels in the hole.

Pollution by Go-Devil Sampler

The concentrations of dissolved lithium (Table 3) are generally quite high and extremely variable for the go-devil samples but not for the Barnes/Uyeda samples. The values in the GDW-III samples are so high that we have little doubt that they reflect contamination by lubriplate grease. M. Mottl (pers. comm., 1983) came to similar conclusions about the Leg 83 samples. Thus, the concentration of each chemical constituent studied in the samples must be evaluated for potential contamination by grease or the packer lubricant.

Minor Constituents

Little hydrogen sulfide was found in the samples, but the concentrations of reduced sulfur compounds are high (Table 4). The Table 4 data and the fairly high concentrations of ammonia suggest that reducing conditions prevail in Hole 504B throughout the depth interval sampled. Whether larger amounts of sulfide did form is at present difficult to assess, because such sulfide might have precipitated in the environment high in dissolved iron. However, anhydrite has been observed in the deeper bentonite samples; thus, a considerable portion, if not all, of the sulfate depletion may be due to $CaSO_4$ precipitation.

The increased concentrations of ammonia may be explained best by both nitrate and nitrogen reduction, such reduction having been catalyzed by the reduced sulfur species or by the presence of iron at high temperature (a process that has been observed before in hydrothermal systems).

Dissolved-silica data from the Barnes/Uyeda *in situ* samples from PAW-2, 3, and 4 are plotted in Figure 6. The concentrations are slightly below the level of quartz saturation in distilled water (Couture, 1977). However, various authors have shown that (at least at 25°C) the solubilities of various silica phases are lower at the ionic strength of seawater by as much as 10%. This hypothesis would indicate that the dissolved silica in the hole is characterized by equilibrium with quartz. The much lower concentrations in the go-devil samples testify to (1) the essential validity of the Barnes/Uyeda samples and (2) the effects of bottom-water contamination as well as the possible re-equilibration with bentonite in the go-devil samples. The concentration of dissolved silica is not clearly correlated with the concentration of dissolved Ca or Mg, so the silica concentrations cannot be used to estimate bottom-water contamination.

Major Constituents

Before discussing major-element correlations we shall discuss the depth distribution of the major cations. For

Table 3. Formation water chemistry.

Sample	Depth (m)	pH (25°C)	Alkalinity (meq/dm^3)	Ca (mM)	Mg (mM)	Li (μM)	Na (mM)	K (mM)	Cl (mM)	SO_4 (mM)	$\Sigma[S^{II-}]$ (μM)	$\Sigma[S_2O_3^{2-}] + [SO_3^{2-}]$ (μM)	Fe^{++} (mM)	SiO_2 (μM)	NO_3 (μM)	NH_4 (μM)	(T°C)	Salinity
BAW-2	564	—	—	16.4	48.4	27	468	10.0	550	28.0	N.D.	N.D.	—	575	0	18	91.5	36.0
BAW-3	650	7.55	1.97	20.1	46.0	37	471	9.1	557	28.0	N.D.	N.D.	—	710	0	20	101	36.3
BAW-4	736	7.49	1.79	23.6	43.2	27	463	9.8	552	26.2	N.D.	1.6	—	905	0	28	108	36.0
BAW-5	1004	7.66	1.94	10.7	53.7	27	473	10.1	552	29.0	—	—	—	155	35	0	130	35.2
GDW-I-1	926	6.36	1.50	28.9	38.9	500	457	8.8	555	22.3	—	—	0.29	680	16.5	72	127	34.6
GDW-I-2	926	6.47	1.415	29.5	37.9	380	446	8.2	555	22.3	—	—	1.08	805	14.5	64	127	34.6
GDW-I-3	926	6.57	1.425	29.4	37.8	175	452	8.2	551	21.2	—	—	1.03	540	5.0	62	127	34.1
GDW-I-4	926	6.39	1.175	28.0	38.2	210	462	8.6	558	21.8	—	—	1.14	535	11.0	69	127	34.1
GDW-I-5	926	6.28	1.26	26.2	39.1	135	460	8.4	552	23.0	N.D.	130	1.24	360	4.0	54	127	34.1
GDW-I-OV	926	6.39	1.185	25.3	41.1	440	464	8.9	553	25.6	—	—	1.01	310	4.5	82	127	34.9
GDW-II-4	1099	6.23	1.55	31.1	34.3	100	450	8.2	556	15.7	1.5	420	1.60	230	2.0	62	141	33.8
GDW-II-5	1099	6.31	1.02	28.1	37.3	75	453	7.9	551	19.6	0.2	320	1.10	145	1.5	59	141	33.8
GDW-II-OV	1099	6.16	0.995	25.3	38.6	115	462	8.4	549	24.0	—	—	—	(130)	0	57	141	34.1
GDW-III-3	1204	6.49	7.57	55.8	20.6	360	408	6.8	526	17.0	—	—	3.71	310	2.5	77	150	33.6
GDW-III-4	1204	6.86	2.70	60.5	20.4	290	433	7.4	563	18.0	—	—	0.33	405	1.0	82	150	35.2
GDW-III-5	1204	7.11	4.05	59.7	23.9	190	433	7.5	566	18.7	N.D.	200	0.46	685	1.0	71	150	36.0
GDW-III-OV	1204	7.19	4.90	60.5	21.1	240	424	7.8	559	15.5	—	—	0.110	1095	1.5	58	150	35.8

Note: OV = overflow chamber. N.D. = not determined; — = not detectable.

Table 4. $(Ca^{2+})(SO_4^{2-})$ ion product in seawater at equilibrium with anhydrite and in Hole 504B samples.

	T (°C)	$(Ca^{2+})(SO_4^{2-})$ $([mM]^2)$
In seawater at equilibrium with anhydrite	25	850
	45	450
	75	300
	125	100
In Hole 504B		
GDW-I	127	620
GDW-II	141	550
GDW-III	150	1022

this we choose magnesium (Fig. 7) as representative because (1) it is removed from any seawater in the hole, presumably into silicates and (2) magnesium depletion due to Mg-oxy-sulfate precipitation should not be a problem at these relatively low temperatures.

We assumed that the NO_3^- concentration of about 15 μM in the GDW-I samples represented pollution by water from the upper part of the hole, and using this value we arrived at a correction for the Mg^{2+} data that suggested lower concentrations *in situ* (Fig. 7). The samples from GDW-II appear to be contaminated by bottom water, despite low NO_3^- concentrations (NO_3^- was probably rapidly reduced in this reducing environment). Bottom-water contamination is also evident from the low dissolved-silica values. The samples from GDW-III, on the other hand, which have a greater bentonite content, are probably much less contaminated by bottom water, although the dissolved-silica values are still low. Figure 7 also shows the magnesium data obtained by Mottl et al. (1985) during Leg 83. The latter data show a considerably larger downhole gradient, but, of course, the hole was much cleaner (less contaminated by bentonite) during Leg 83, and the hole had been left for a longer time span for reaction.

We conclude that the *in situ* data probably follow a smooth trend line, a result in part of decreased reaction rates at higher levels (lower temperatures) in the hole and a result also of mixing effects in the hole.

In the following discussion we assume that one type of reaction sequence is responsible for both the release of calcium by volcanic rocks and the uptake of magnesium, potassium, and sodium. This assumption appears to be in reasonable agreement with the experimental work of Seyfried and Bischoff (1979). If this hypothesis is true, the relationships between major-ion concentrations would be nearly linear. If downhole mixing is also important, as suggested by the Barnes/Uyeda samples, linear relationships would also occur.

Major-Ion Correlations

Figure 8 presents a correlation plot of Ca^{2+} versus Mg^{2+}. The solid dots are measured values. Only the Barnes/Uyeda samples and the samples from go-devil runs GDW-I and GDW-II show a 1:1 correlation between calcium and magnesium. Some of the factors that have a bearing on these data are discussed below.

The detection of measurable amounts of anhydrate in the lower parts of the hole strongly suggests that substantial amounts of $CaSO_4$ have precipitated. As discussed earlier, little evidence had been found for sulfide formation, at least in major quantities, although reduced sulfur compounds do occur (Table 3). We have, therefore, assumed that much of the sulfate has been removed from the waters as a result of anhydrite precipitation.

From the literature, we obtained (Ca^{2+}) (SO_4^{2-}) ion products in seawater solutions in equilibrium with anhydrate (Table 4). The ion products for Hole 504B water samples are also listed in Table 4. At all depths the solubility product is exceeded and thus precipitation is theoretically possible.

Assuming that all sulfate depletion is the result of calcium sulfate precipitation, we can compute a corrected calcium concentration as follows:

$$Ca_{corrected} = Ca_{measured} + \Delta SO_4$$

where ΔSO_4 is the change in sulfate concentration from seawater (about 29 mM). The corrected data are plotted in Figure 8. The uncertainty in SO_4 is probably ± 2 mM at most, that in Ca ± 1 mM; thus, we estimate the corrected values to be within 5% of those given.

Both sodium (obtained from change balance calculations) and potassium show decreases with increasing depth (Table 3). In Figure 9 these data are plotted versus Mg^{2+}. For a drop in Mg^{2+} of about 32 mM (52.5 to 20.5 mM), there is a change in Na^+ of about 50 mM and in K^+ of about 3 mM. If we assume that the corrected Ca^{2+} values are representative of the Ca^{2+} increase, one obtains a slope of $\Delta Ca^{2+}/\Delta Mg^{2+} = -1.9$, or a change in Ca^{2+} of about 61 mM for a drop in Mg^{2+} of 32 mM. Thus, if the total anion concentration is approximately constant, one needs $2 \times (61 - 32) = 58$ mM of Na^+ and K^+ to compensate the net Ca^{2+} gain, in very good agreement with observed changes. It is probable that Na^+ uptake is due to Na^+–montmorillonite formation, an idea also suggested by bentonite alteration in Hole 504B.

For comparison we present in Figure 8 the Leg 83 extrapolated values for Ca^{2+} and Mg^{2+} (Mottl et al., 1985). These data follow our suggested correlation.

Summary and Conclusions

1. Originally introduced surface seawater in the hole has been entirely displaced by displaced by bottom water as a result of mixing processes along a density gradient. Such mixing, which may well be a continuous process, explains in part the apparently smooth gradients in chemical composition down the hole, although the increased reaction rates at the increasing downhole temperatures will also contribute to this process. We suggest that bottom-water chlorinities have been established throughout the hole by slow downward mixing, but that reaction rates involving cation exchange with basalts and bentonite are rapid enough to establish gradients in the major-ion composition.

2. Dissolved-silica concentrations may be controlled by quartz solubility.

3. Dissolved-nitrate values suggest that waters from the upper part of the hole are introduced to greater depths

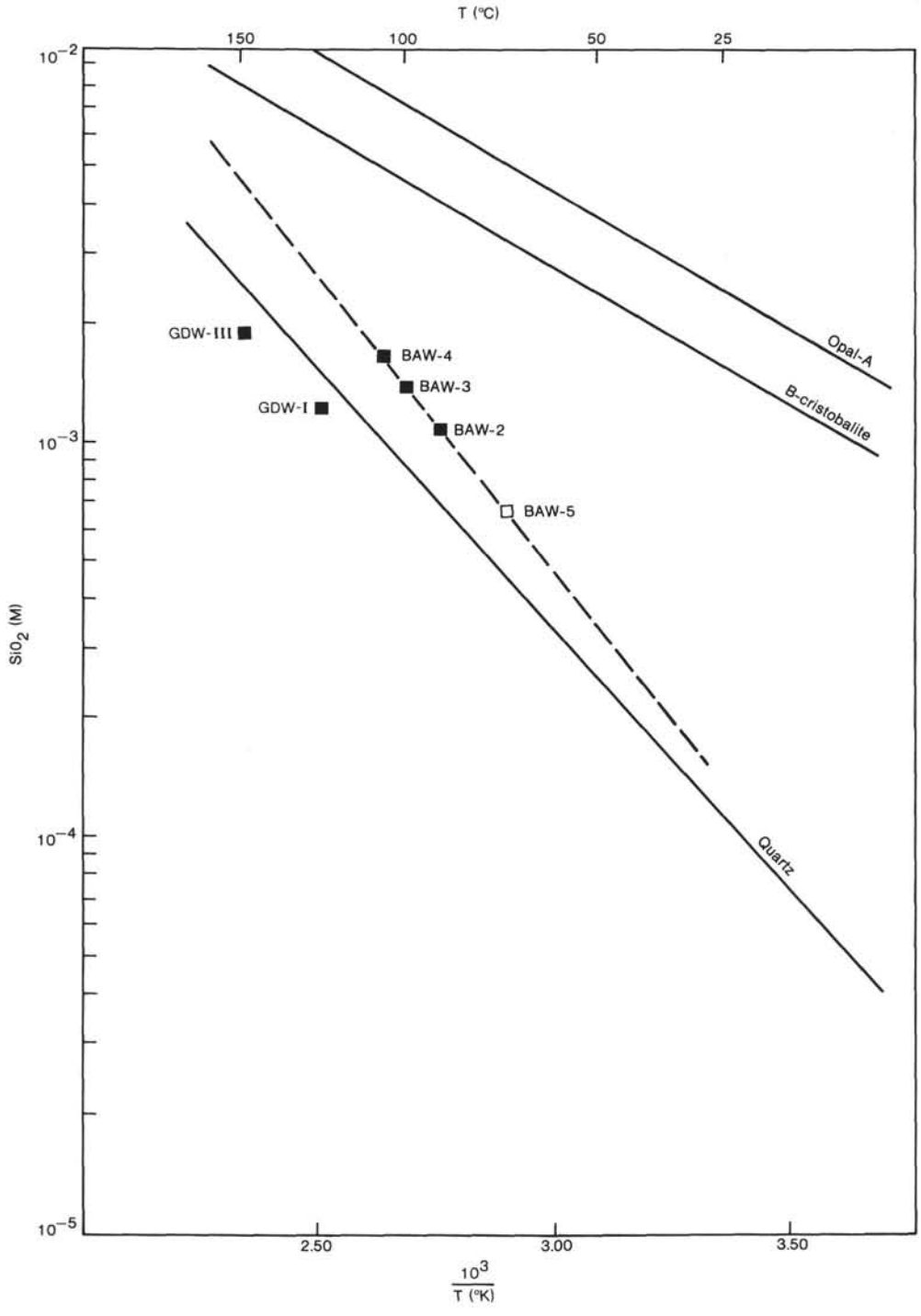

Figure 6. Dissolved silica versus temperature, Hole 504B. Solid lines are solubility curves determined by Couture (1977).

as a result of the downdraft created by lowering the drill pipe and/or the sampler. This water has caused contamination in the go-devil samples and in one Barnes/Uyeda sample.

4. Ammonia may result from nitrate and/or nitrogen conversion catalyzed by high concentrations of dissolved iron.

5. Close correlation between calcium (after adjustment for anhydrite precipitation) and magnesium suggests a slope of $\Delta Ca/\Delta Mg = -1.9$, the excess calcium produced being balanced by Na^+ and K^+ uptake.

TEMPERATURE MEASUREMENTS

Hole 504B, spudded during Leg 69 in October 1979, has been re-entered on three subsequent legs: Leg 70 (December 1979), Leg 83 (November 1981 to January 1982), and Leg 92 (April 1983). In each case an important priority upon re-entry was the measurement of borehole

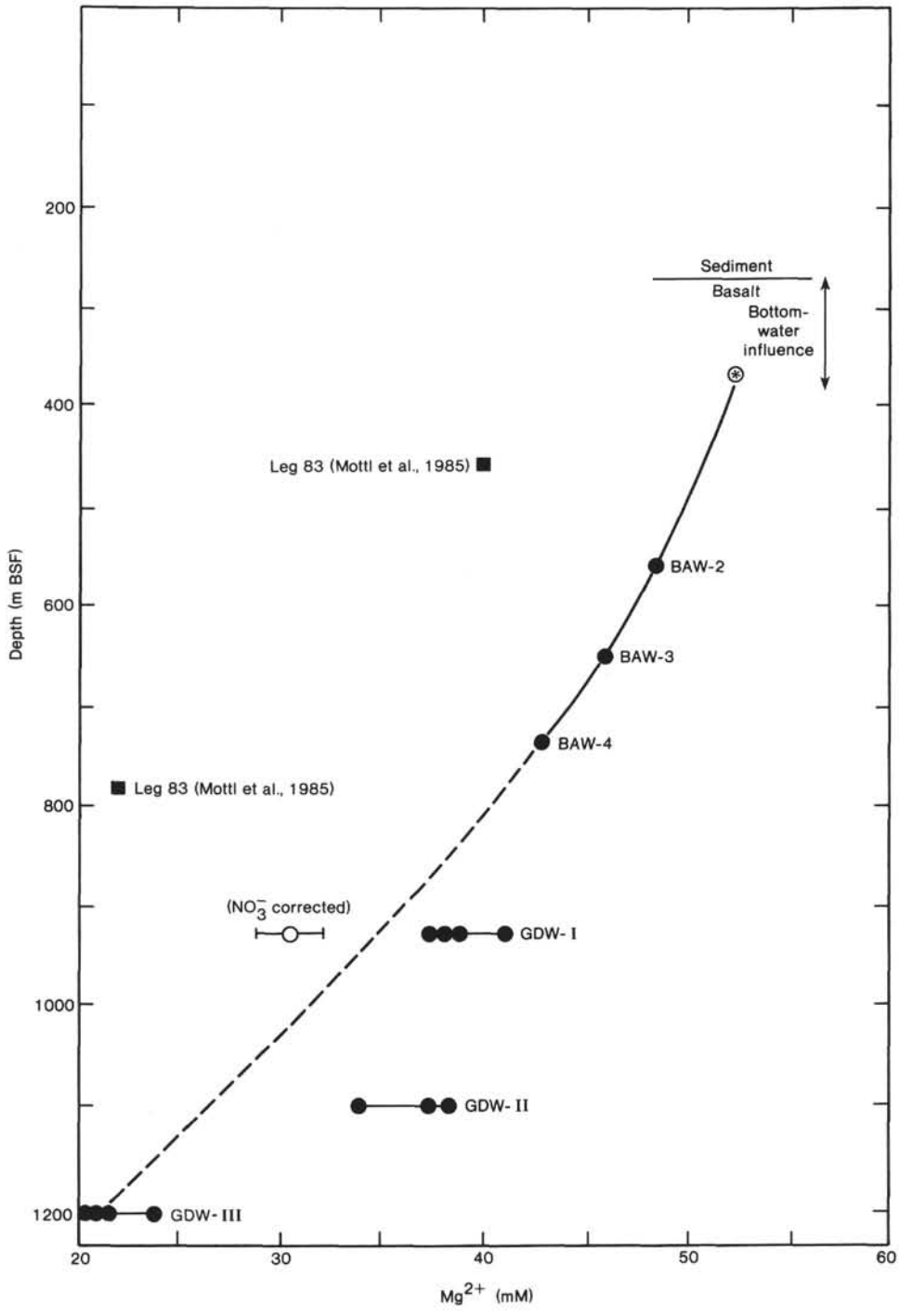

Figure 7. Dissolved magnesium versus depth, Hole 504B. Dashed line represents suggested Mg^{2+} values after correction for contamination by water from higher in the hole.

temperatures, before any disturbance of the water in the hole (Fig. 10). The periods of time between the four legs were sufficiently long so that the disturbances to the borehole temperatures due to drilling operations on previous legs should have dissipated, and borehole temperatures should have fully equilibrated with geothermal conditions. The first order of business after the re-entry of Hole 504B on Leg 92 was the acquisition of a sequence of temperature measurements and water samples. These measurements were made in steps down the hole, with no pumping. The results are assumed to represent the equilibrium downhole thermal state.

Extensive temperature logging during Legs 69, 70, and 83 (Becker, Langseth, and Von Herzen, 1983; and Becker, Langseth, Von Herzen, and Anderson, 1983) revealed an extraordinary downhole flow of ocean bottom water into a shallow basement reservoir, superimposed on a predominantly conductive geothermal gradient extending from 400 to 1350 m BSF (Fig. 10). Becker et al. (both 1983 refs. cited above) based the following conclu-

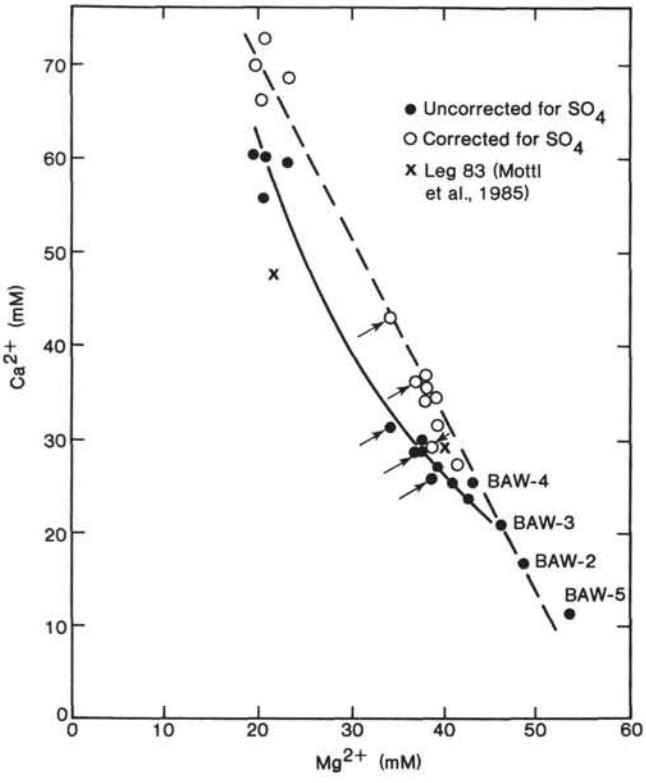

Figure 8. Dissolved calcium versus magnesium, Hole 504B. Arrows identify samples before and after correction. Solid line connects uncorrected data; dashed line connects corrected data.

sions on these temperature measurements: (1) the rate of downhole flow was on the order of 90 m/hr. (6000 l/hr.) in December 1979 and had decreased to about 25 m/hr. (1500 l/hr.) by November 1981; (2) the downhole flow was directed into a high permeability (greater than 60-mD) reservoir that probably encompassed the upper 100 m of basement; and (3) before Hole 504B was drilled, heat transfer through the upper 1.35 km of ocean crust there was predominantly conductive and in agreement with the theoretical value of about 190 mW/m^2 predicted from plate cooling models. The temperature measurements showed no clear evidence that hydrothermal circulation is presently active in the vicinity of Hole 504B; the downhole flow after drilling was not hydrothermal convection, but was flow forced by basement pore fluid underpressures (Anderson and Zoback, 1982).

The Leg 92 temperature measurements were designed to reassess the two major hydrogeologic/geothermal processes occurring in the hole. We particularly wanted to know (1) the April 1983 rate of downhole flow to find out whether the flow rate had continued to decay since Leg 83 (as we expected); and (2) the equilibrium geothermal gradient in the deep basement, particularly in the section drilled by Leg 83 (836 to 1350 m BSF), where no undisturbed temperatures had been measured previously. We were successful in meeting our first goal, but only partially successful in determining the deep geothermal gradient, primarily because of the difficulty of accurately measuring the very high downhole temperatures (about 100 to 160°C). The temperature measure-

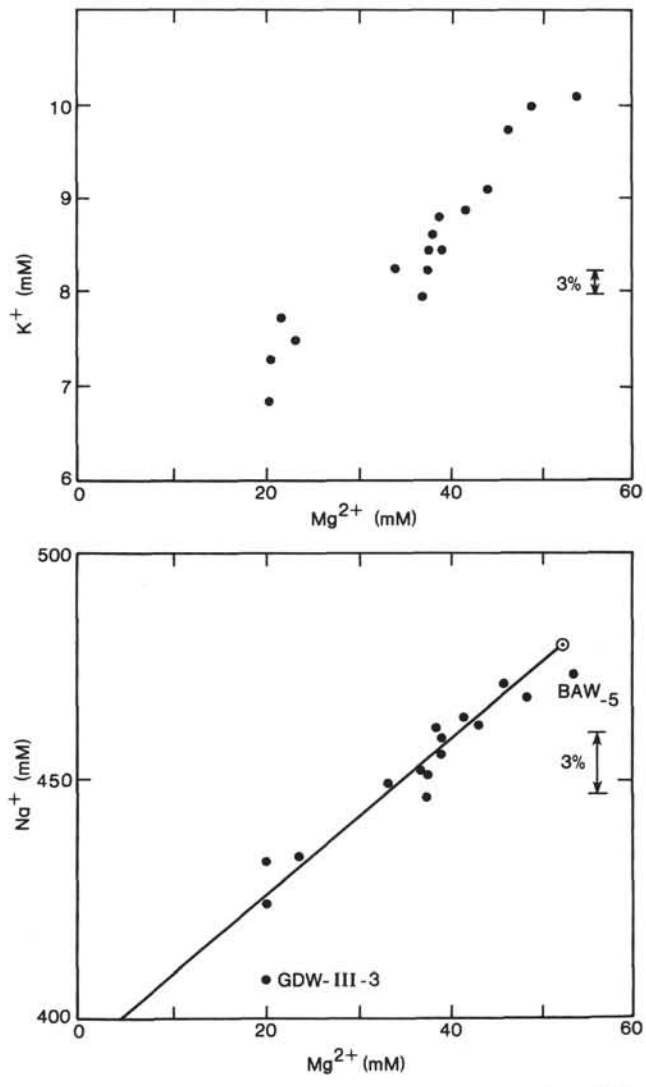

Figure 9. Dissolved potassium and sodium versus magnesium, Hole 504B.

ments in Hole 504B from Legs 69, 70, 83, and 92 are discussed in detail by Becker et al. (1985).

Measurement Techniques

The sequence of temperature measurements in Hole 504B during Leg 92 is summarized in Table 5. Three different devices were used to measure temperatures: (1) the Barnes/Uyeda *in situ* pore water heat flow sampler, which was a modification of a design by Yokota et al. (1980); (2) the Von Herzen hydraulic piston corer (HPC) heat flow shoe; and (3) maximum-reading thermometers. Both the Barnes/Uyeda probe and the HPC shoe monitor the resistance of single thermistors, which on Leg 92 were fixed 1.3 and 1.1 m in front of the bit. The Barnes/Uyeda probe records 128 resistance samples at user-selected 1- or 2-min. intervals; the HPC tool was set to record 1379 samples at 12-s intervals. Every tool was allowed to free fall to the bit instead of being lowered while attached to a wire line. This allowed us to add sections of pipe while the temperatures were being measured, so we were able to measure temperatures over a

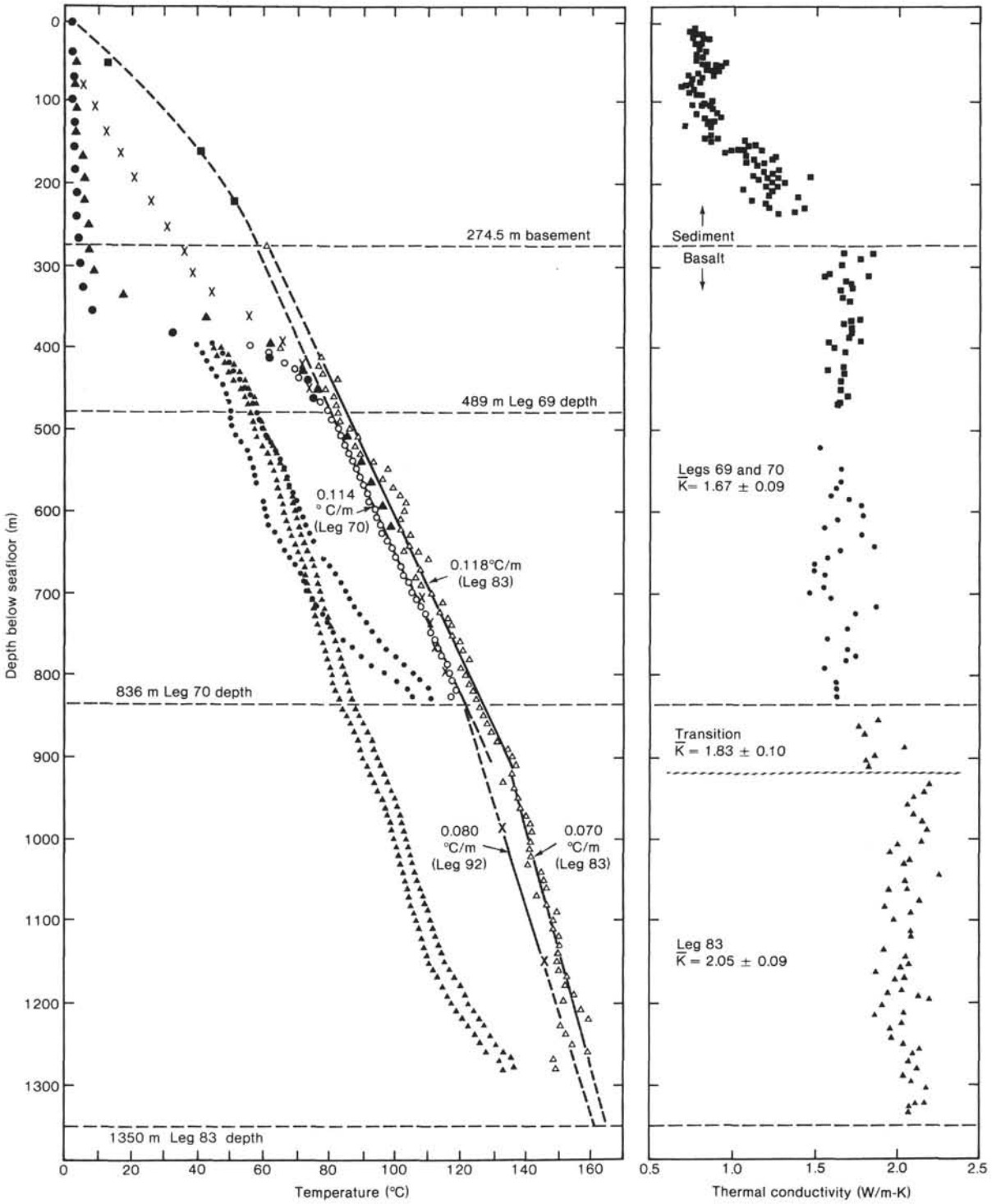

■ Hole 504C sediment temperatures, Leg 69

Equilibrium re-entry temperatures, Hole 504B

● Leg 70 (measured 3 Dec. 1979)

▲ Leg 83 (measured 23 Nov. 1981)

X Leg 92 (measured 8 Apr. 1983; HPC and Barnes/Uyeda probe)

Temperatures measured after drilling disturbance and extrapolations to equilibrium, Hole 504B

• Leg 70 temperatures

○ Leg 70 extrapolation to equilibrium

▲ Leg 83 temperatures

△ Leg 83 extrapolation to equilibrium

Figure 10. Temperatures and thermal conductivities measured at Site 504 during Legs 69, 70, 83, and 92 (Becker et al., 1985). Temperatures are from Hole 504B except as noted; sediment thermal conductivities are from Hole 504. $\bar{K}$ is average thermal conductivity. Dashed lines are extrapolations of linear gradients, which are shown as solid lines where well determined.

Table 5. Leg 92 temperature measurements, Hole 504B.

Heat flow lowering	Tools used	Depth (m BSF)	Number of temperature–depth data	Remarks
8	Von Herzen HPC heat flow shoe	77.9–449.3	12	Excellent data quality to 70°C
	Barnes/Uyeda probe[a]	77.9–449.3	14	Good data quality
9	Barnes/Uyeda probe[a]	478.0–563.6	4	No data transferred to read-out box
10	Barnes/Uyeda probe[b]	563.6–678.5	5	Recorder drift—minimum *in situ* value was acquired at 563.6 m[d]
11	Barnes/Uyeda probe[c]	707.3–793.5	4	Good data quality
	Maximum-reading thermometer	793.5	1	Thermometer reading: 115°C
	Large-volume water sampler with one maximum-reading thermometer	926.4	1	Broken thermometer
12	Barnes/Uyeda probe[c]	985.2–1033.2	3	Recorder drift—minimum *in situ* value was acquired at 985.2 m[e]
	Maximum-reading thermometer	1033.2	1	Faulty thermometer—readings were too high
	Three maximum-reading thermometers in heat flow assembly	1050.9	1	Two thermometers were faulty; one measured 133.3°C[f]
	Large-volume water sampler with three maximum-reading thermometers	1099.8	1	Two thermometers were questionable;[g] one measured 134.7°C[h]
13	Barnes/Uyeda probe	1146.7	1	Recorder drift—minimum *in situ* value was acquired at 1146.7 m
	Large-volume water sampler with two maximum-reading thermometers	1204.3	1	One thermometer was questionable;[g] one measured 142.2°C[h]

[a] Recorder no. 1, set for normal (low) temperatures. Thermistor #6.
[b] Recorder no. 2, adjusted for high temperatures. Thermistor #6.
[c] Recorder no. 1, adjusted for high temperatures. Thermistor #6.
[d] Strong temperature effect on recorder response—recorded temperatures drift too low with time. Maximum value was obtained at first depth, before temperature effect became too significant.
[e] Moderate temperature effect on recorder response—recorded temperatures drift too low with time. Maximum value was obtained at first depth, before temperature effect became too significant.
[f] 100-to-400°F thermometer in pressure case. Mercury separated during measurement. Unable to shake down and reuse thermometer.
[g] Thermometer was exposed, requiring pressure correction to high indicated values.
[h] 0-to-300°F thermometer in pressure case.

depth interval greater than the length of a stand of pipe. A typical tool run included several 8- to 10-min. stops at intervals of single stands of pipe (about 28.5 to 29 m).

Both the Barnes/Uyeda probe and the HPC heat flow shoe were run simultaneously during a single lowering in the upper part of the hole (0 to 450 m), where the downhole flow of bottom water was expected to depress temperatures and no borehole water samples were desired. We used two tools to guarantee the recovery of data in this interval so we would be sure to be able to estimate the downhole flow rate. The Barnes/Uyeda data were good throughout the lowering, and the HPC data were superb (Fig. 11) except for the last two temperatures, which were too high for the 0-to-70°C range of the HPC thermistor bridge. At every depth the temperatures from the two tools agreed within 2%; above 30°C, the Barnes/Uyeda readings were consistently lower than the HPC heat flow tool values. Since the HPC thermistor had been calibrated more recently, and since the HPC tool recorded the known bottom-water temperature (2.01°C) very accurately, the HPC readings were assumed to be accurate and were used to determine the flow rate. For the two measurements above 70°C, where the HPC tool was off scale, the Barnes/Uyeda values were corrected by +1.9%, the average ratio of the HPC values to the Barnes/Uyeda probe values in the range from 30 to 70°C.

Below 400 m, temperatures greater than 70°C precluded the use of the HPC temperature tool, and the Barnes/Uyeda probe was run for short intervals (Fig. 12). The Barnes/Uyeda recorder was adjusted to increase the resolution of the thermistor's resistance (which is low at high temperatures). Several factors limited the accuracy of the Barnes/Uyeda readings at temperature greater than 100°C:

1. Thermistor resistance was calibrated only to 100°C. The validity of extrapolating the calibration constants to higher temperatures is unknown.

2. At high temperatures, relatively large changes in temperature produce only small changes in thermistor resistance, so the nominal resolution of the recorder is limited to about ±0.5 to 1°C.

3. The recorder electronics are sensitive to high temperatures, as indicated by the obvious downward drift of temperatures with time at heat flow stations 10, 12, and 13 (Fig. 12). Because of this effect, the highest values yielded at these stations are those recorded first (at the shallowest depths, immediately after the tool free fell to the bit), and even these values are considered min-

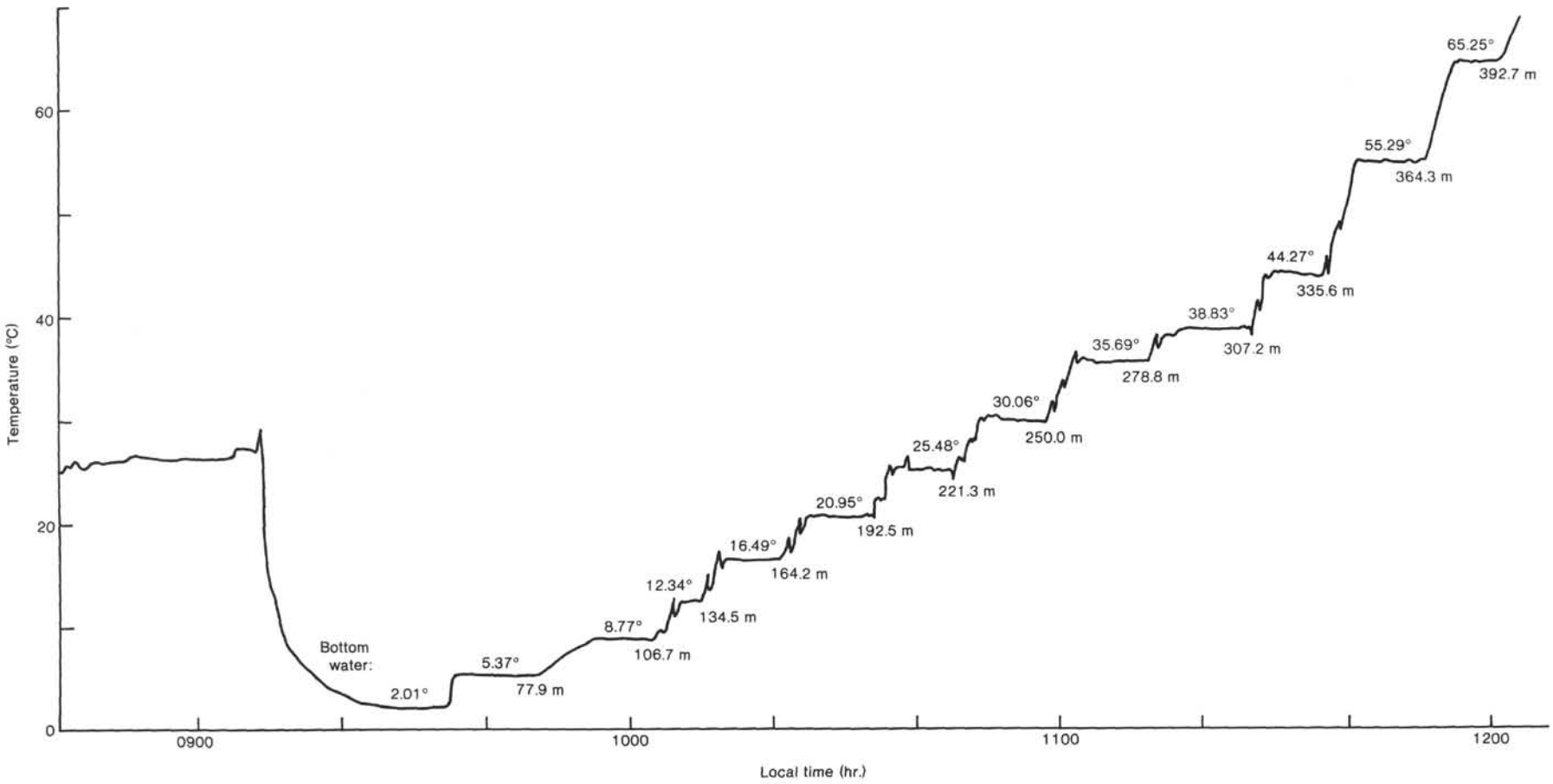

Figure 11. Temperatures measured with the Von Herzen HPC heat flow shoe during the first Leg 92 temperature lowering in Hole 504B (8 Apr. 1983). Depths are in m BSF. The Barnes/Uyeda probe record for the same lowering is shown in Figure 12.

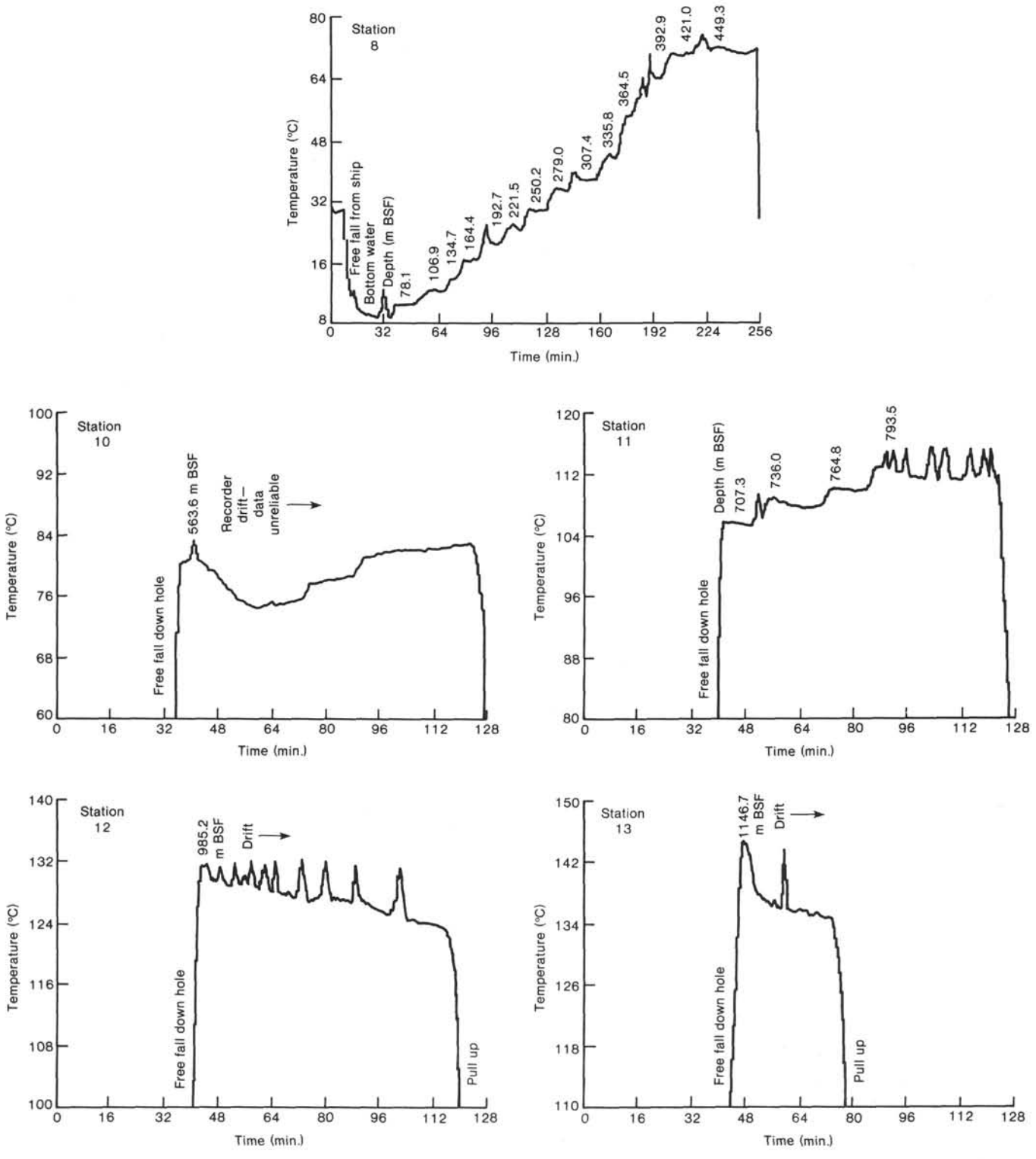

Figure 12. Temperature–time records for the successful Leg 92 Barnes/Uyeda probe lowerings in Hole 504B (Leg 92 heat flow/pore water stations 8, 10, 11, 12, 13). Occasional spurious temperature spikes are probably the result of missed digits in the recorded thermistor resistances. Note the drift of the recorder response in three of the deeper, higher temperature stations (10, 12, and 13). For these three stations, the maximum recorded temperature was interpreted as a minimum value for the *in situ* temperature.

imum for the depth being measured, because the free fall was largely through cold bottom water, with only a few minutes of the descent through the warm water in the hole.

The recorder used for most of the stations (no. 1) was the one that showed less drift (sensitivity to temperature). However, it was also noisier and occasionally dropped digits during recording or playback. Many of the dropped digits could be corrected, but those that could not probably produced the narrow spikes in the records shown in Figure 12. During a distilled-water boiling-point calibration of the Barnes/Uyeda probe, the probe read 99.5 to 99.9°C. Nevertheless, because of the factors discussed above, the accuracy of the Barnes/Uyeda probe measurements is probably no better than ±2 to 3°C at temperatures above 100°C.

Several maximum-reading thermometers were used in water-sampler lowerings between temperature stations (Table 5). Over half of the thermometers run produced no usable data because of breakage and the effects of pressure. Two thermometers produced reasonable data in the bottom of the hole, but only one could be shaken down and reused. The latter was tested in a distilled-water boiling-point calibration, and it read 100 to 100.5°C, but it was later broken and so cannot be tested at higher temperatures. Despite the fact that both this thermometer and the Barnes/Uyeda probe calibrated very well at 100°C, the downhole readings from the two differed by 5 to 10°C at higher temperatures. We have greater confidence in the readings from the previously reliable Barnes/Uyeda probe, which gave higher downhole temperatures than the maximum-reading thermometers. Our bias is supported by the chemistry of the water obtained by the large-volume samples in which the maximum-reading thermometers were run. The nitrate concentrations suggest that cold bottom water was brought into the hole around the sampler, resulting in measured temperatures cooler than geothermal temperatures.

Results

The undisturbed Leg 92 hole temperatures are shown along with the Leg 69, 70, and 83 results in Figure 10. Above 400 m, the Leg 92 data provide a good indication of the downhole flow rate. Deeper than 400 m, the Leg 92 values are generally consistent with a conductive heat transfer of about 190 mW/m^2, but this conclusion is not unequivocally supported by temperatures obtained in the section drilled on Leg 83 (900 to 1350 m BSF).

Leg 92 Rate of Flow of Bottom Water Down Hole 504C

As on Legs 69, 70, and 83, the temperatures measured in the casing (0–275 m) and in the uppermost basement are significantly lower than those expected both from the surface heat flow and from the sediment temperatures measured at Hole 504C (Fig. 10). The low temperatures indicate the continued downhole flow of bottom water into the upper section of basement. The temperatures measured in the cased section during Leg 92 are clearly higher than those measured on Leg 83, which were in turn higher than the values measured on Leg 70. The increase in temperature indicates a significant slowing in the rate of downhole flow over the more than 3 yr. since the flow started (when Leg 69 first drilled into basement).

Becker et al. (both 1983 refs.) developed a complicated model to predict the temperatures that would occur down the casing as the result of various uniform (steady-state) rates of flow. This model considers only steady-state flow rates and yields estimates of upper bounds for the real, decaying flow rates. The Leg 70 data indicated a flow rate on the order of 90 m/hr. (about 6000 l/hr.), and the Leg 83 data 2 yr. later indicated a flow rate of 25 m/hr. (about 1500 l/hr.). An exponential fit through these two flow rate estimates suggested that the Leg 92 flow rate would be on the order of 10 to 15 m/hr. When the high-quality Leg 92 HPC temperature data are plotted over the temperature profiles predicted by Becker for several constant flow rates (Fig. 13), however, the Leg 92 temperatures indicate an even lower flow rate than expected, on the order of 2 to 3 m/hr. (100 to 200 l/hr.).

The downhole flow has been shown to be forced by underpressures in the upper part of basement (Anderson and Zoback, 1982). However, the origin of these underpressures has not been determined. The strong decrease in flow rate over 3 yr. (Fig. 14) may result from several factors: (1) a local decrease in the magnitude of the underpressures in the vicinity of the hole; (2) local

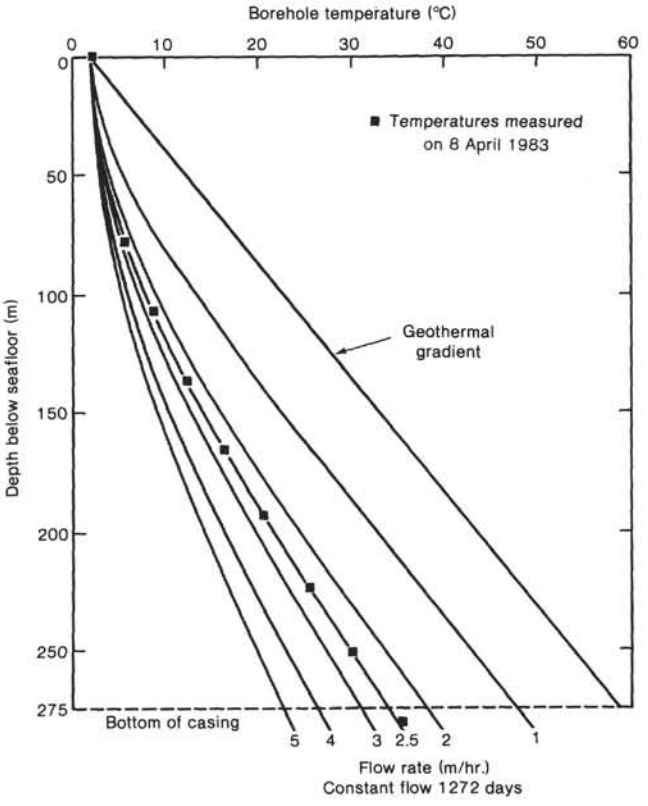

Figure 13. Leg 92 re-entry temperature measurements in the upper part of Hole 504B, plotted on predicted temperature profiles for the downhole flow of bottom water at a constant rate since October 1979 (1272 days), when Leg 69 penetrated basement.

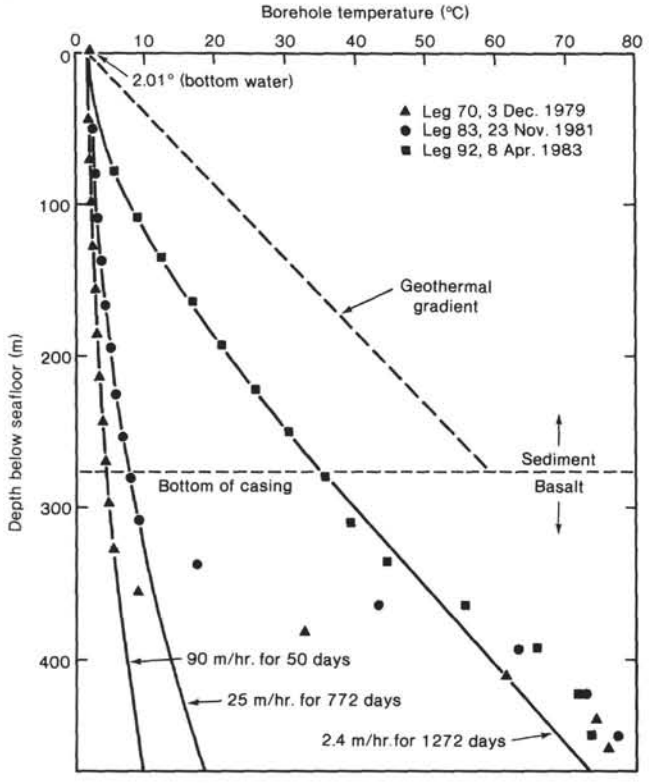

Figure 14. Leg 70, 83, and 92 equilibrium re-entry temperatures and best-fit theoretical profiles for constant flow rates. The sharp increase in temperatures at about 350 to 370 m indicates that virtually no flow continued deeper.

changes in the permeability near the hole, possibly resulting from chemical reactions between basalt and the flowing seawater; and/or (3) the filling of a relatively small reservoir (on the order of 1 km in radius) into which Hole 504B was drilled.

Deep Basement Heat Flow

The downhole flow of ocean bottom water extends only about 100 m into basement and is an artifact of drilling through the sediment seal; it has had no noticeable effect on temperatures deeper than 400 m, which are representative of the pre-drilling geothermal state of the crust. Two types of temperature data exist below 400 m: undisturbed temperatures (those measured immediately upon the re-entry of the hole on Legs 70, 83, and 92), and paired (continuous temperature logs taken at the end of Legs 69, 70, and 83). The latter temperatures were measured in the borehole after it had been disturbed by the drilling process, but undisturbed temperatures can be estimated by extrapolation (by using the method of, for example, Bullard, 1947).

In work based largely on such extrapolations and confirmed by the equilibrium re-entry temperatures at depths shallower than 650 m, Becker et al. (both 1983 refs.) concluded that conductive heat transfer predominates in the basement at Hole 504B. In the 400- to 900-m section, linear gradients of about 0.11°C/m were indicated by both the Leg 70 and Leg 83 extrapolated temperatures, although the results of the two legs were offset by about 5° (Fig. 10). Becker, Langseth, Von Herzen, and Anderson (1983) and Becker et al. (1985) prefer the lower (Leg 70) values, because the data quality was poorer on Leg 83 and the Leg 83 drilling disturbance of the hole was much more complicated and harder to compensate for. Below 900 m, a steplike increase in thermal conductivity associated with a transition from pillow lavas to dikes produced a lower temperature gradient of about 0.07°C/m (Fig. 10).

An important goal of the Leg 92 re-entry temperature measurements was to verify the extrapolation of the basement temperatures and to test the linearity of the predominantly conductive temperature gradient, particularly at depths below 900 m. As shown by Figure 10, the Leg 92 temperatures generally corroborate the linear temperature gradient of 0.11°C/m in the pillow lavas above 900 m, and they support the interpretation that the Leg 83 extrapolated temperatures were about 5° too high.

At depths greater than 900 m, the five Leg 92 temperature measurements show considerable scatter, primarily because three different devices were used to obtain the data: the Barnes/Uyeda probe (two measurements) and two maximum-reading thermometers. However, the scatter in the data does not suggest other than a conductive, linear gradient. We estimate this gradient by differencing each of the two data pairs measured with a single instrument. The preferred Barnes/Uyeda probe readings yield a gradient of 0.080°C/m; the maximum-reading thermometer data yield a gradient of 0.072°C/m. The maximum-reading thermometer temperatures seem about 5 to 10°C low, whereas the Barnes/Uyeda probe readings extrapolate nicely to meet the better quality data above 900 m. Extrapolating the Barnes/Uyeda gradient deeper indicates a bottom-hole temperature of 160 to 165°C.

Thus, we interpret the sketchy Leg 92 data below 900 m as indicating slightly lower temperatures than the Leg 83 estimated temperatures and as having a slightly (5 to 10%?) higher gradient. This interpretation, if accurate, would partially resolve an otherwise unexplained discrepancy in the Leg 83 data: although there is clearly a change in the linear gradients of the Leg 83 estimated temperatures at 900 m that is associated with a discontinuity in thermal conductivity across the pillow–dike transition, the heat flow values that are calculated from these gradients do not agree particularly well with each other. Becker, Langseth, Von Herzen, and Anderson (1983) estimated a heat flow of 180 ± 20 mW/m^2 for depths from 400 to 900 m and a heat flow of 140 ± 30 mW/m^2 for depths greater than 900 m. A slightly higher gradient below 900 m would result in a heat flow value that would be in better agreement with both that calculated for the section above and that predicted for the plate (about 190 mW/m^2). Specifically, the Barnes/Uyeda probe temperatures below 900 m, which give a gradient of 0.08°C/m, result in a heat flow estimate of 160 mW/m^2 (see Becker et al., 1985, for detailed discussion).

According to the analysis of Luheshi (1983), the conductive gradient deeper than 400 m is clearly large enough to allow slow convection and mixing of the fluids within the borehole. Such convection would be unrelated to the

downhole flow of ocean bottom water into the upper 100 m of basement. Such convection must also be slow enough so that a conductive gradient within the borehole could be maintained by radial conduction in equilibrium with the geothermal gradient in the surrounding crust. Such possible convection could have important implications for the interpretation of the chemistry of sampled borehole fluids.

MULTICHANNEL SONIC LOGGING AND PACKER EXPERIMENT

For the last several years, the Lamont-Doherty Geological Observatory and the U.S. Geological Survey at Menlo Park have been making *in situ* geophysical measurements of the properties of the oceanic crust that most directly affect the circulation of an active hydrothermal system penetrated by Hole 504B, which is on the southern flank of the Costa Rica Rift (Anderson et al., 1982). Measurements of permeability, ultrasonic borehole imagery, and two-channel Schlumberger sonic logging have provided a most useful description of the changes in the circulation of oceanic crust Layers 2A, 2B, and 2C that are related to the degree of fracturing and alteration. However, Layer 2A is so intensely fractured that the attenuation of sonic energy was too great to cross-correlate the two waveforms returned from each shot by the Schlumberger tool. It is precisely this attenuation that marks the zones of highest permeability in the oceanic crust. We returned to Hole 504B during Leg 92 to run a multichannel sonic log through Layer 2A. Our tool has two major advantages over the Schlumberger sonic log: (1) the spacing between the receivers is 1 ft. (0.30 m) instead of 2 ft. (0.61 m), and (2) the tool has eight receivers instead of two. The eight receivers allow us to develop a small refraction profile across the array at each shot depth. Precise velocities and waveform spectra are recorded across the array. Deeper into the dikes of Layer 2C, we found that the rock had distinctive filter characteristics. Wavelengths of 30 to 40 cm were severely attenuated for both the P and S coda. We interpreted this spacing as being related to the aspect ratio of a fundamental pattern of fracturing or jointing never before observed in oceanic crust. We were anxious to determine the filter characteristics of Layer 2A in Hole 504B.

A unique aspect of our logging program is the construction of a fracture spectrum log of the hole. In this log we display the degree of fracturing observed on the borehole televiewer with the P and S wave velocity and the P and S coda peak frequency and energy. An alteration log designed to distinguish between the porosity and the hydroxyl content of the formation (which uses a nuclear log cross-correlation technique developed at Lamont) adds the downhole variation in the degree of alteration downhole to the observed acoustic changes.

Operations

A detailed description of the multiple-receiver, long-spacing sonic logging tool and operating techniques appears in the Site 597 chapter (this volume).

The 12-channel receiver array for the multichannel sonic logging tool, which was severely damaged at Site 597, was repaired and reassembled as an 8-channel string, with spacing as follows: source to first receiver, 10.3 ft. (3.14 m); receiver 1 to receiver 2 and receiver 2 to receiver 3, 1 ft. (0.30 m); receiver 3 to receiver 4, 2 ft. (0.61 m); receiver 4 to receiver 5, 1 ft. (0.30 m); receiver 5 to receiver 6, 2 ft. (0.61 m); receiver 6 to receiver 7 and receiver 7 to receiver 8, 1 ft. (0.30 m). This reconstruction was important, because a new 12-channel array that was shipped to Costa Rica was impounded by customs at San José, so we sailed from Puntarenas, Costa Rica, on the *Ellen B. Scripps* for the rendezvous with the *Glomar Challenger* without the replacement array.

The tool was first put down the hole on 14 April, and it worked beautifully. However, software looping and uphole computer triggering problems prevented the proper recording of waveforms. The interval from 3850 to 3750 m below the rig floor (376.5 to 276.5 m BSF) was logged onto floppy disks. Later playback revealed no useful information on the disks. The software program was digitizing part of the first waveform eight times. We spent the next 2 days attempting to debug the program and planning alternative recording techniques. We decided to record the data on video tape and Polaroid images from an oscilloscope. The program was eventually debugged and used to digitize from the videotape playback. When we again logged Hole 504B from 3900 to 3750 m (426.5 to 276.5 m BSF), the tool functioned beautifully; in total, 400 sonic waveforms were recorded during 1.5 hr. in the formation.

Results

A description of the advantages of multichannel sonic logging can be found in the Site 597 chapter (this volume). In brief, recording a source with a less-than-1-m wavelength by using eight receivers spaced 1 ft. (0.3 m) apart produces waveforms sensitive to borehole changes that occur over less-than-0.3-m intervals. Fractures, pillow boundaries, flow contacts, and so forth can be seen as differences between coda (waveform packets) over several receivers. These changes in P, S, Stonely, and late-arriving normal modes can be related directly to the borehole televiewer image (BHTV). Because the tool was stationary at each shot point (shot points were 3 m apart), a miniature refraction survey resulted from each shot. The waveforms are displayed in Figure 15. Table 6 lists the changes observed in the waveform coda that relate directly to the downhole changes in the BHTV images (which were logged during Leg 83).

The results are excellent. The traveltimes of the P and S coda are highly erratic in Layer 2A in the previous Schlumberger log, but the normal moveout of P and S coda across our MCS logging array allow us to make precise velocity calculations at each shot depth. The system also makes possible the observation of changes in both the amplitude and frequency of the normal modes—particularly the shear and Stonely waves. Attenuation can be calculated by measuring the amplitude and frequency changes of these coda between waveforms. It

Table 6. Comparison between multichannel sonic waveforms (Fig. 15) and borehole televiewer imagery (Newmark et al., 1985) in Hole 504B.

Depth below rig floor (m)	Depth below seafloor (m)	Observations on Leg 92 multichannel sonic logs	Observations on Leg 83 borehole televiewer imagery
3751	277.5	Variation in amplitude across receiver array. Change in frequency of shear and Stonely coda. Channels 6, 7, 8 have high frequency reflections? or normal modes.	Zone of internal fracturing.
3754	280.5	Change in amplitude across receiver array.	Fracturing at positions of receivers 6 to 8.
3757	273.5	Largest amplitudes at middle receivers (5 and 6).	Position of middle receivers corresponds to zone of unfractured rock between fractured zones.
3760	286.5	Amplitude changes from low to high down string.	Fractured zone at receivers 1 to 3. Rock is more solid at receivers 4 to 8.
3763	289.5	Change in modal coda (three packets at receiver 3, two at receiver 2).	Massive basalt.
3766	292.5	Large variation in amplitudes of shear code.	Fractured zone.
3772	298.5	Very fast: wave at receiver 8 is 1 to 2 km/s faster than it was at 3766 m.	Massive.
3775	301.5	Repeatability of waveforms shown on multiple shots at receivers 5 and 6.	Massive.
3778	304.5	Large coda change across receiver array.	Rubble zone.
3781	307.5	Amplitude increases at receiver 8.	Rubble zone to massive at 3783 m (309.5 m BSF).
3784	310.5	Receiver 7 charging against wall.	Massive basalt with fractures.
3787	313.5	Saturated amplitudes.	Massive—no fractures.
3790	318.5	Saturated amplitudes, very fast shear.	Massive—no fractures.
3793	312.5	Still saturated.	Massive—no fractures.
3796	324.5	Boundary in amplitude between receivers 5 and 6.	Fractured but more massive, deeper than receiver 5.
3799	327.5	On first receiver, highest coda amplitude is shear rather than Stonely (which are high frequency and slow).	Rubble zone, heavily fractured zone.
3802	330.5	Low amplitude at receivers 2 and 3. High amplitude at receivers 5 and 6. High frequencies on receiver 7.	Breccia.
3805	331.5	Highest amplitude at receiver 4. Low frequency Stonely coda.	Aquifer.
3808	334.5	High frequency Stonely coda. No shear coda except at receiver 1.	Aquifer.
3811	337.5	High shear amplitude on receiver 1. Change in shear velocity and amplitude below receivers 2 and 3.	Aquifer.
3817	343.5	Ultra-high-frequency Stonely coda.	Aquifer.
3820	346.5	Highest frequencies at receiver 4, lowest at receiver 7.	End of aquifer; then into fractured basalt.
3823	349.5	Larger shear than Stonely coda. Very low frequency Stonely coda at receiver 8.	Extensively fractured.
3826	352.5	Receiver 1, huge amplitude; receiver 2, two coda packets; receiver 3, no large shear.	Extensively fractured.
3835	361.5	Stonely velocity, 6 km/s.	Positive zones spaced at about 5-m intervals.
3838	364.5	Shear velocity, 1.23 km/s.	Fractured zone.
3841	367.5	Clear P coda at receiver 1.	Still fractured.
3844	370.5	P velocity very slow, about 1.5 km/s.	Heavily fractured.
3847	373.5	Low amplitude at receiver 8.	Small breccia zone at receiver 8.
3850	376.5	Shear velocity, 1.8 km/s.	Vertical fractures.
3853	379.5	Attenuation strong at receiver 8.	Fractured zone.
3856	382.5	Saturated at receivers 4 to 5. Different shear factor at receiver 8 than at receiver 7.	Fractured zone.
3859	385.5	Large shear velocity jump of 0.6 km/s between receivers 5 and 6. Then receiver 8 faster than receiver 6.	Small solid flow at 3861 m (387.5 m BSF).
3862	388.5	P velocity, 3.7 km/s.	Extensively fractured.
3865	391.5	Larger amplitudes at receivers 3 to 6, then small again at receivers 7 to 8.	Extensively fractured.
3868	394.5	Large shear coda at receiver 1.	Extensively fractured.
3871	397.5	Saturated amplitudes at receiver 5.	Extensively fractured.
3883	409.5	Shear velocity, 2.4 km/s.	Solid flow at 3880 to 3885 (406.5 to 411.5 m BSF).
3886	412.5	Large P coda, velocity 2 to 4 km/s at receivers 1 to 3 but 4.3 km/s at receivers 7 to 8.	Rubble to fractured basalt.
3889	415.5	P wave velocity up to 2.8 km/s.	Fractured basalt.

should be noted that the tool makes a downhole correction for geometric attenuation by automatically increasing the gain at successively more distant receivers. No intrinsic attenuation would give eight waveforms with exactly the same energy and frequency content for each coda. Fractures clearly affect attenuation by scattering and venting energy away from the borehole. Shipboard (preliminary) observation of the waveforms leads us to believe that this scattering is the dominant mode of attenuation in the upper oceanic crust (not a surprising result). Table 6 reveals a direct correlation between the degree of fracturing and the degree of attenuation in Layer 2A.

Packer Experiment

For the third time at Hole 504B, we attempted to make a packer slug flow test of permeability at 4530 m below rig floor (1056.5 m BSF) in the dikes at the bot-

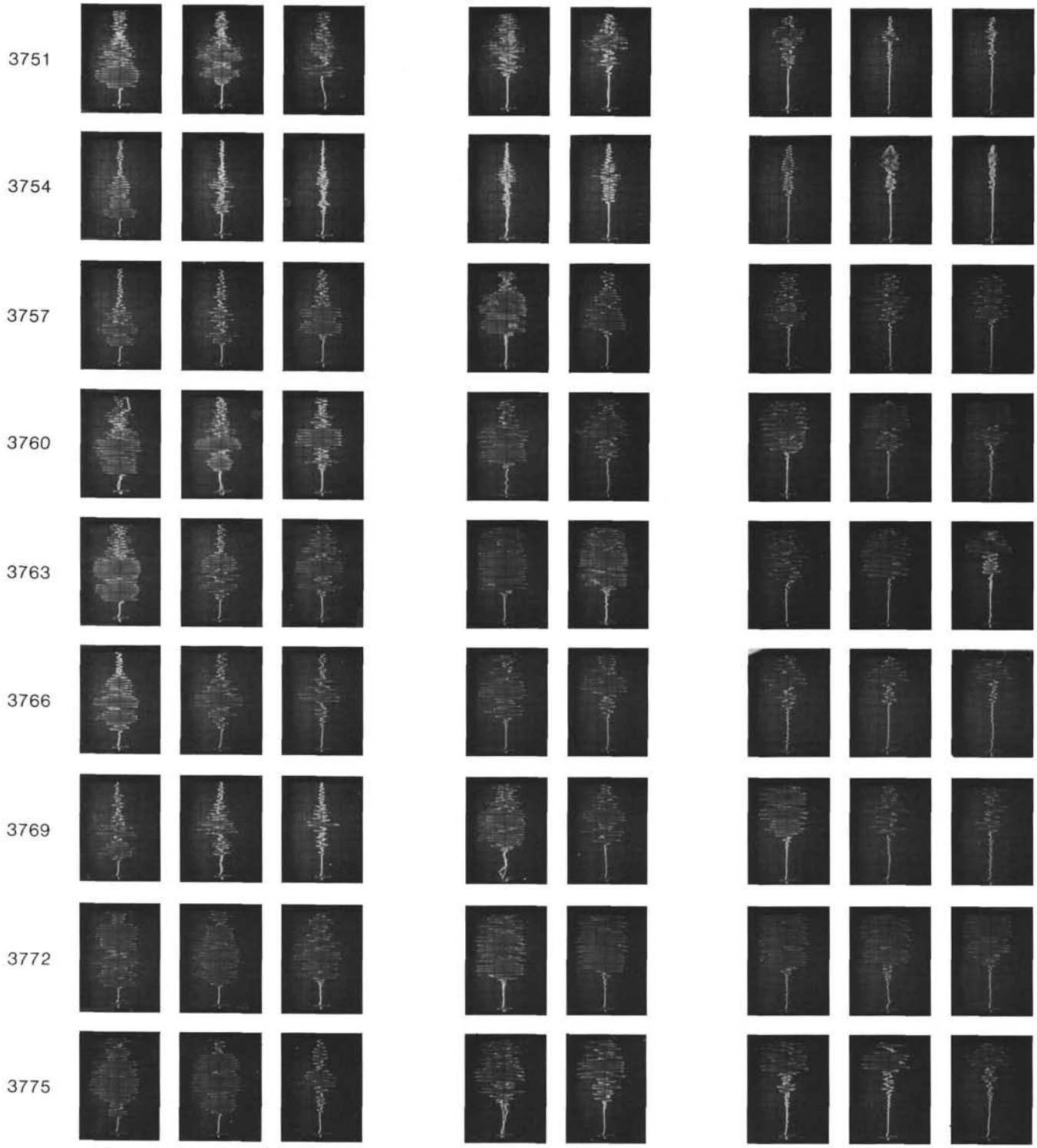

Figure 15. Full waveforms recorded by the multichannel sonic logging tool. At each depth, signals recorded from the near receiver (farthest left) to the far receiver (farthest right) are shown. The eight receivers are spaced from 3 to 6 m from the source (see text). Typical frequencies are from 5 to 20 kHz, and typical traveltimes over the offset spread are from 50 to 200 μs/ft. (164 to 656 μs/m).

tom of the hole. A permeability of 10^{-19} m^2 was expected at this depth as the result of calculations based upon the exponential decrease in measured permeability with increasing depth shallower in the hole. However, the packer jacket failed at the high temperatures encountered in the dikes. We have now shown conclusively that the DSDP packer system will not work at 150°C. Two failures were identified. The one-way check valve on the go-devil that prevents deflation when the go-devil shear plug blows out returned to the surface damaged, and the packer element itself returned stripped of its outer rubber tread. The steel belt showed enough damage to suggest that the

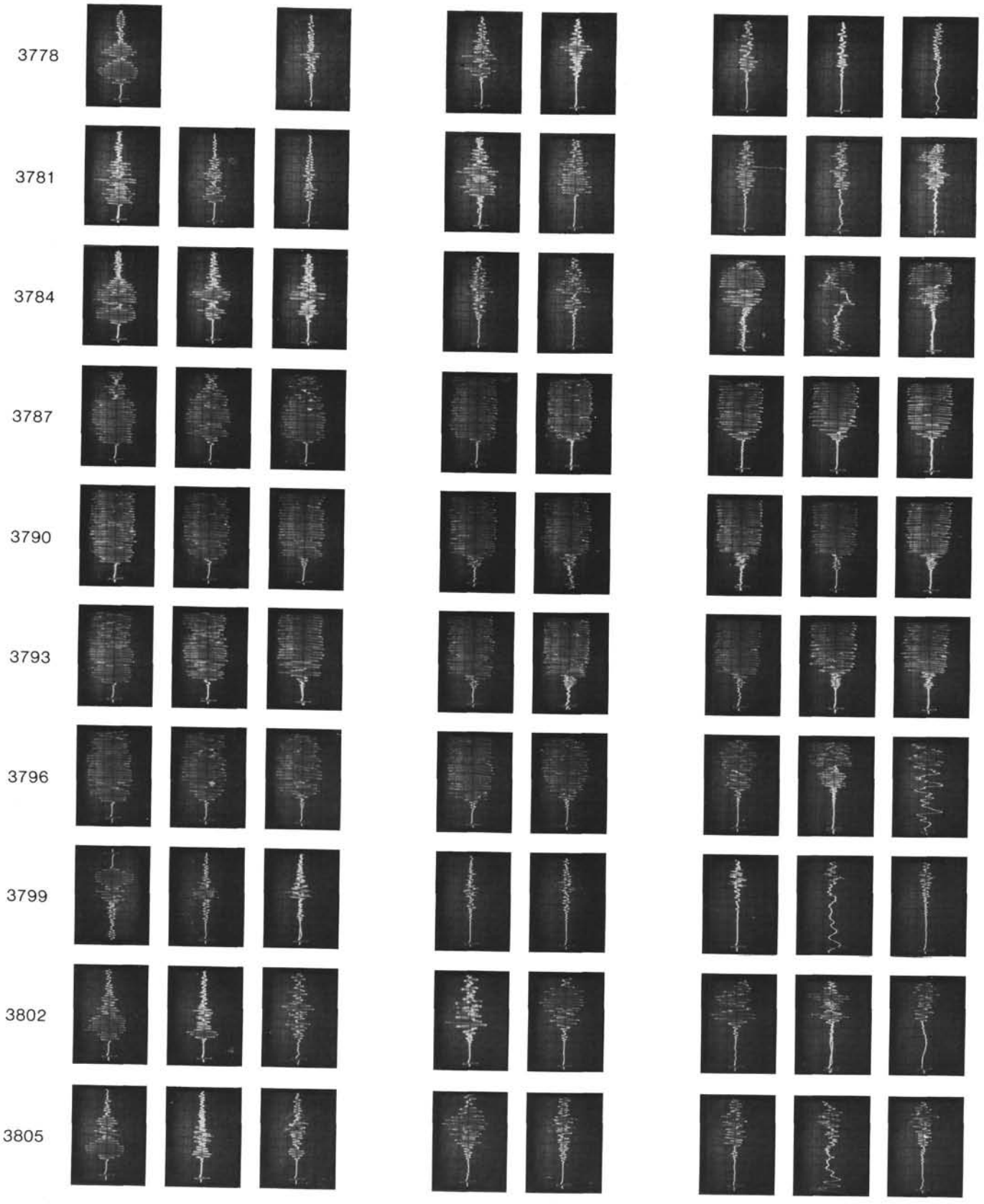

Figure 15 (continued).

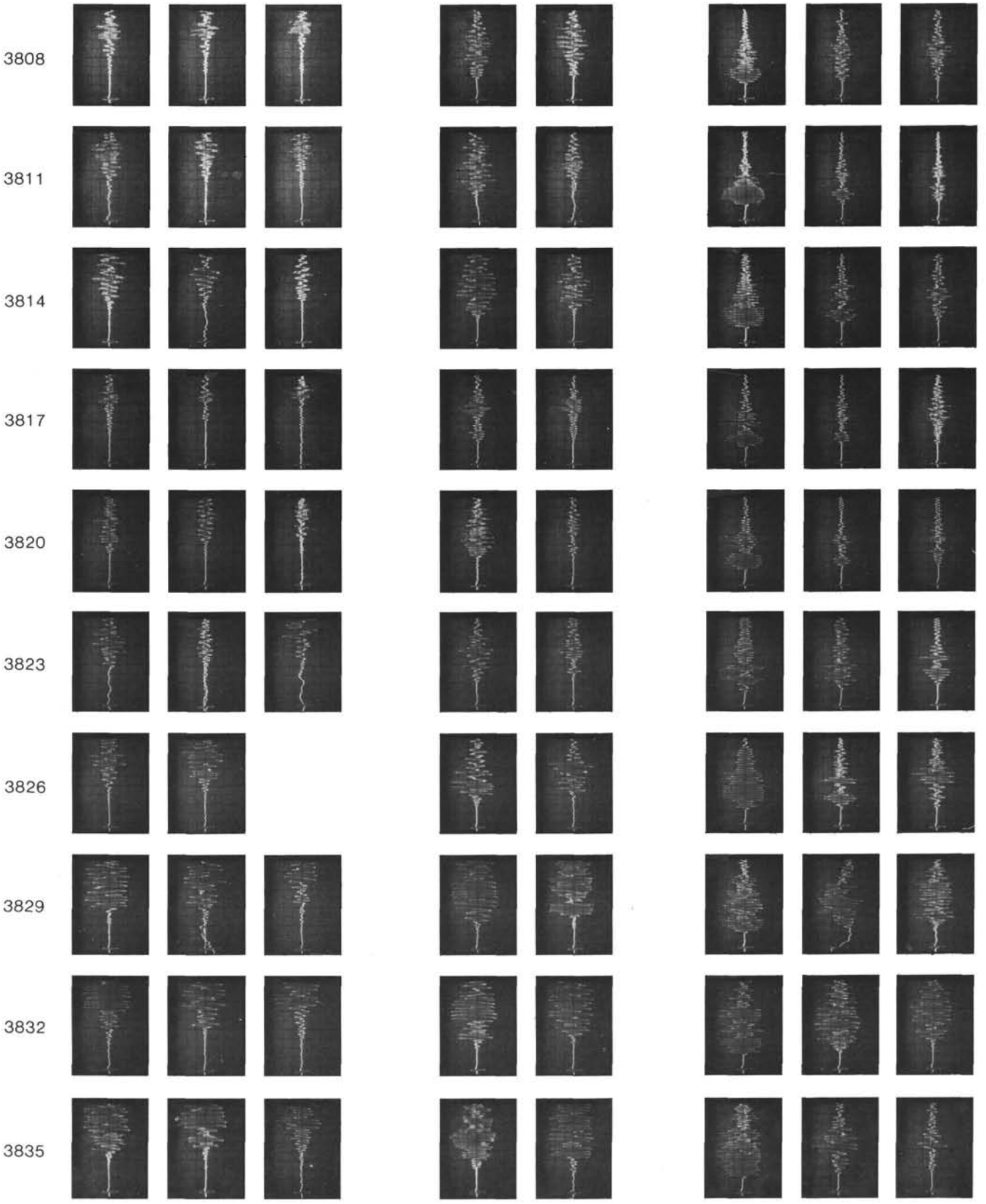

Figure 15 (continued).

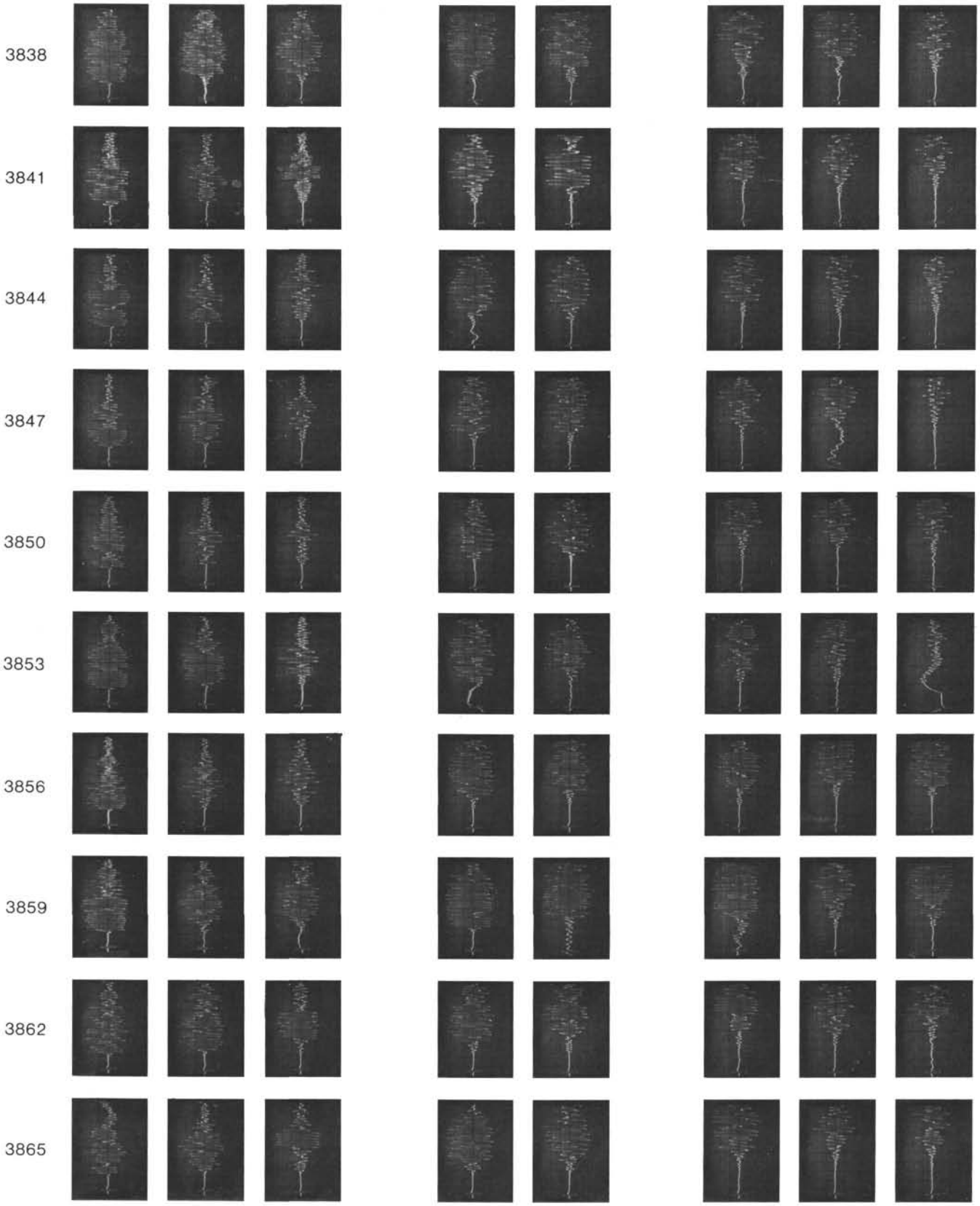

Figure 15 (continued).

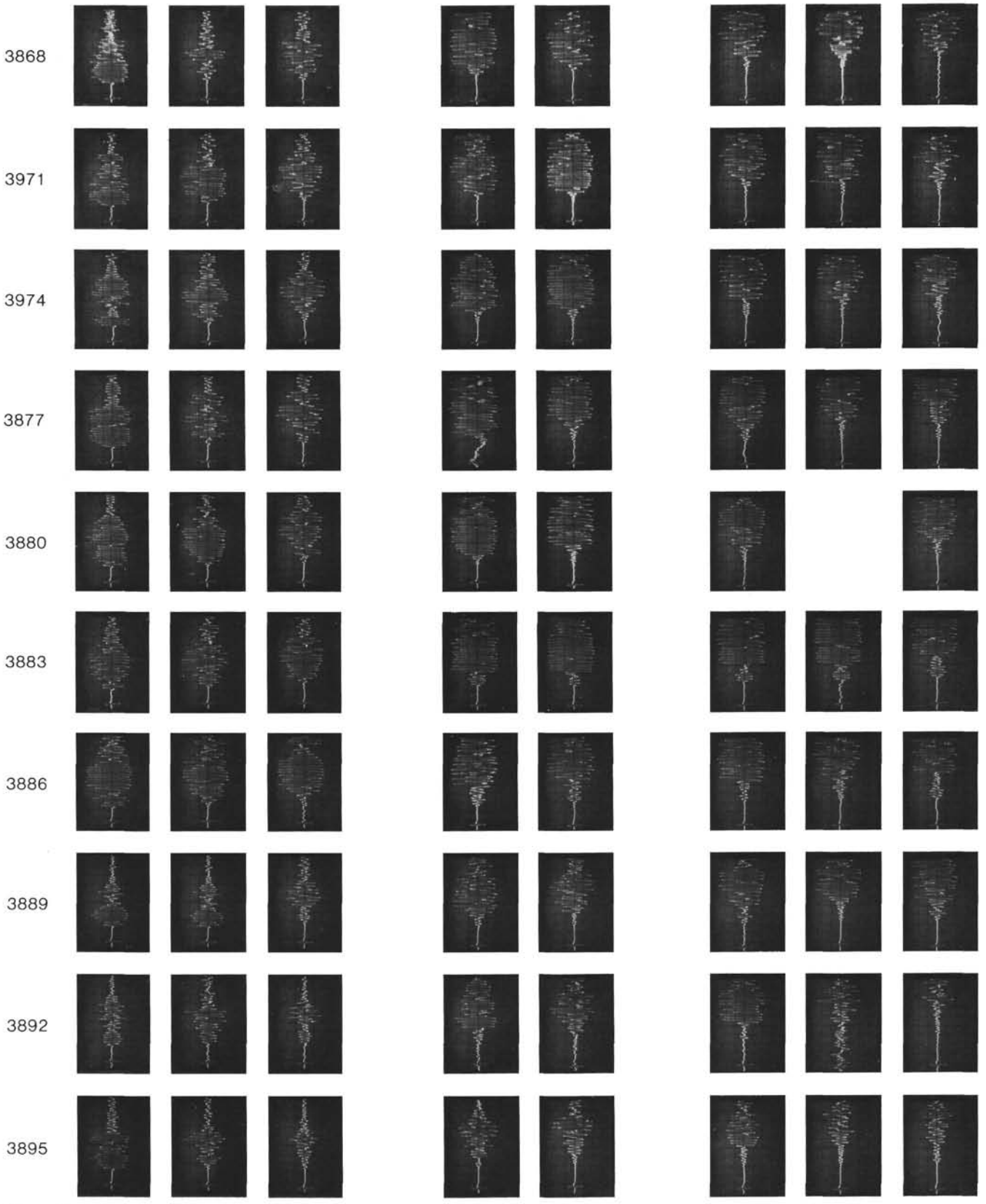

Figure 15 (continued).

tread was already gone at the point of inflation. The steel slammed against the borehole and failed to hold a hydraulic seal even momentarily. The next alternative appears to be to try asbestos packers.

SUMMARY AND CONCLUSIONS

A number of sampling and measurement programs were conducted at Hole 504B at the end of Leg 92. Extensive temperature logging during Legs 69, 70, and 83 showed a rate of downhole water flow of 90 m/hr. in December 1979, which decreased to 25 m/hr. in November of 1981. The flow was directed to an underpressured high permeability reservoir in the upper 100 m of basement. Leg 92 temperature measurements showed that the flow had decreased to 2 or 3 m/hr., or 100 to 200 l/hr., by April of 1983. Downhole temperature measurements were complicated by sensor problems but indicate a gradient of 0.080°C/m in crustal Layer 2C with bottomhole temperatures of 160 to 165°C (Becker et al., 1985).

Water sampling showed the borehole fluid in Hole 504B in April of 1983 to be a mixture of seawater and bentonite drilling mud. We found uniform bottom-water chlorinites down the hole but a clearly developed major-ion alteration chemistry characterized by downhole increases in Ca^{2+} and decreases in Mg^{2+} and K^{+}. The good correlation between Ca^{2+}, after adjustment for the anhydrite precipitation observed lower in the hole, and Mg^{2+} suggests a value of -1.9 for the Ca/Mg ratio. Dissolved-silica concentrations follow the quartz solubility curve.

Dr. Ralph Stephen of the Woods Hole Oceanographic Institution conducted an oblique seismic refraction experiment in which shots fired at the surface were registered by a three-component seismometer clamped to the borehole wall at depths of 317 m BSF, 547 m BSF, 727 m BSF, and 942 m BSF. The *Ellen B. Scripps* was the shooting ship. The experiment was designed to investigate regional fracture density, seismic anisotropy, and low velocity layers. Data analysis is incomplete, but the Leg 92 borehole seismic experiment is the most comprehensive completed to date, even though cable connector failures plagued the experiment. The preliminary data show clear evidence of anisotropy (Little and Stephen, 1985).

Sections of the upper portion of Hole 504B were logged with a multichannel sonic tool to interpret mesoscale fracturing from the acoustic behavior of crustal Layer 2A in the immediate vicinity of the borehole. A comparison of the results of this logging with the results of previous borehole televiewer logging shows that the differences in the shape of the waveforms correspond to differences in the degree of fracturing. A packer experiment intended to determine the bulk formation permeability deep in the hole failed because the rubber borehole seal could not withstand the high ambient temperatures.

During two intervals between other operations we pumped 150,000 gal. of seawater through the hole from a below rig floor depth of 4734 m (1270 m BSF). We estimate that this procedure is equivalent to 6.8 flushings and thus should have removed 99% of the bentonite not caked on the walls of the hole.

REFERENCES

Anderson, R. N., and Hobart, M. A., 1976. The relation between heat flow, sediment thickness, and age in the eastern Pacific. *J. Geophys. Res.*, 81:2968–2989.

Anderson, R. N., Hobart, M. A., and Langseth, M G., 1979. Geothermal convection through oceanic crust and sediments in the Indian Ocean. *Science*, 204:828–832.

Anderson, R. N., Honnorez, J., Becker, K., et al., 1985. Hole 504B. *In* Anderson, R. N., Honnorez, J., Becker, K., et al., *Init. Repts. DSDP*, 83: Washington (U.S. Govt. Printing Office), 13–67.

Anderson, R. N., Honnorez, J., Becker, K., Adamson, A. C., Alt, J. C., et al., 1982. DSDP Hole 504B, the first reference section over 1 km through Layer 2 of the oceanic crust. *Nature*, 300(5893): 589–594.

Anderson, R. N., and Zoback, M. D., 1982. Permeability, underpressures, and convection in the oceanic crust near the Costa Rica Rift, eastern equatorial Pacific. *J. Geophys. Res.*, 87:2860–2868.

Becker, K., Langseth, M. G., and Von Herzen, R. P., 1983. Deep crustal geothermal measurements, Hole 504B, Deep Sea Drilling Project Legs 69 and 70. *In* Cann, J. R., Langseth, M. G., Honnorez, J., Von Herzen, R. P., White, S. M., et al., *Init. Repts. DSDP*, 69: Washington (U.S. Govt. Printing Office), 223–236.

Becker, K., Langseth, M. G., Von Herzen, R. P., and Anderson, R. N., 1983. Deep crustal geothermal measurements, Hole 504B, Costa Rica Rift. *J. Geophys. Res.*, 88:3447–3457.

Becker, K., Langseth, M. G., Von Herzen, R. P., Anderson, R. N., and Hobart, M. A., 1985. Deep crustal geothermal measurements, Hole 504B, Deep Sea Drilling Project Legs 69, 70, 83, and 92. *In* Anderson, R. N., Honnorez, J., Becker, K., et al., *Init. Repts. DSDP*, 83: Washington (U.S. Govt. Printing Office), 405–418.

Bullard, E. C., 1947. The time necessary for a bore hole to attain temperature equilibrium. *Mon. Not. R. Astron. Soc., Geophys. Suppl.*, 5:127–130.

Cann, J. R., Langseth, M. G., Honnorez, J., Von Herzen, R. P., White, S. M., et al., 1983. *Init. Repts. DSDP*, 69: Washington (U.S. Govt. Printing Office).

Couture, R. A., 1977. Synthesis of some clay minerals at 25°C; palygorskite and sepiolite in the oceans [Ph.D. dissert.]. Univ. Calif., San Diego.

Gieskes, J. M., 1983. The chemistry of interstitial waters of deep sea sediments: Interpretation of deep sea drilling data. *In* Riley, J. P., and Chester, R. (Eds.), *Chemical Oceanography* (Vol. 8): London (Academic Press), 221–269.

Gieskes, J. M., and Lawrence, J. R., 1981. Alteration of volcanic matter in deep sea sediments: evidence from the chemical composition of interstitial waters from deep sea drilling cores. *Geochim. Cosmochim. Acta*, 45:1687–1703.

Lawrence, J. R., and Gieskes, J. M., 1981. Constraints on water transport and alteration in the oceanic crust from the isotopic composition of pore water. *J. Geophys. Res.*, 86:7924–7934.

Lawrence, J. R., Gieskes, J. M., and Broecker, W. S., 1975. Oxygen isotope and cation composition of DSDP pore waters and the alteration of Layer II basalts. *Earth Planet. Sci. Lett.*, 27:1–10.

Little, S. A., and Stephen, R. A., 1985. Costa Rica Rift borehole seismic experiment, Deep Sea Drilling Project Hole 504B, Leg 92. *In* Anderson, R. N., Honnorez, J., Becker, K., et al., *Init. Repts. DSDP*, 83: Washington (U.S. Govt. Printing Office), 517–528.

Luheshi, M. N., 1983. Estimation of formation temperature from borehole measurements. *Geophys. J. R. Astron. Soc.*, 74:747–776.

McDuff, R. E., 1981. Major cation gradients in DSDP interstitial waters: the role of diffusive exchange between seawater and upper oceanic crust. *Geochim. Cosmochim. Acta*, 45:1705–1713.

Mottl, M. J., Druffel, E. R. M., Hart, S. R., Lawrence, J. R., and Saltzman, E. S., 1985. Chemistry of hot waters sampled from basaltic basement in Hole 504B, Deep Sea Drilling Project Leg 83, Costa Rica Rift. *In* Anderson, R. N., Honnorez, J., Becker, K., et al., *Init. Repts. DSDP*, 83: Washington (U.S. Govt. Printing Office), 315–328.

Newmark, R. L., Anderson, R. N., Moos, D., and Zoback, M. D., 1985. Sonic and ultrasonic logging of Hole 504B and its implications for the structure, porosity, and stress regime of the upper 1 km of the oceanic crust. *In* Anderson, R. N., Honnorez, J., Becker, K., et al., *Init. Repts. DSDP*, 83: Washington (U.S. Govt. Printing Office), 479–510.

Seyfried, W. E., Jr., and Bischoff, J. L., 1979. Low temperature basalt alteration by seawater: an experimental study at 70°C and 150°C. *Geochim. Cosmochim. Acta*, 43:1937–1947.

Stephen, R. A., 1977. Synthetic seismograms for the case of the receiver within the reflectivity zone. *Geophys. J. R. Astron. Soc.*, 51: 169–181.

_____, 1978. The oblique seismic experiment in oceanic crust [Ph.D. dissert.]. Dept. Geodesy and Geophysics, Madingley Rise, Cambridge University, United Kingdom.

_____, 1979. The oblique seismic experiment in oceanic crust—equipment and technique. *Mar. Geophys. Res.*, 4:213–226.

_____, 1981. Seismic anisotropy observed in upper oceanic crust. *Geophys. Res. Lett.*, 8:865–868.

_____, 1983. The oblique seismic experiment on Deep Sea Drilling Project Leg 70. *In* Cann, J. R., Langseth, M. G., Honnorez, J., Von Herzen, R. P., White, S. M., et al., *Init. Repts. DSDP*, 69: Washington (U.S. Govt. Printing Office), 301–308.

Stephen, R. A., and Harding, A. J., 1983. Travel time analysis of borehole seismic data. *J. Geophys. Res.*, 88:8289–8298.

Stephen, R. A., Johnson, S., and Lewis, B., 1983. The oblique seismic experiment on Deep Sea Drilling Project Leg 65. *In* Lewis, B. T. R., Robinson, P., et al., *Init. Repts. DSDP*, 65: Washington (U.S. Govt. Printing Office), 319–328.

Stephen, R. A., Louden, K. E., and Matthews, D. H., 1980a. The oblique seismic experiment on Deep Sea Drilling Project Leg 52. *In* Donnelly, T., Francheteau, J., Bryan, W. B., Robinson, P., Flower, M., Salisbury, M., et al., *Init. Repts. DSDP*, 51, 52, 53, Pt. 1: Washington (U.S. Govt. Printing Office), 675–704.

_____, 1980b. The oblique seismic experiment on DSDP Leg 52. *Geophys. J. R. Astron. Soc.*, 60:289–300.

Yokota, T., Kinoshita, H., and Uyeda, S., 1980. New DSDP (Deep Sea Drilling Project) downhole temperature probe utilizing IC RAM (memory) elements. *Tokyo Daigaku Jishin Kenkyujo Iho*, 55:75–88.